European Journal of Pharmaceutics and Biopharmaceutics 150 (2020) 50–65

Contents lists available at ScienceDirect

European Journal of Pharmaceutics and Biopharmaceutics

journal homepage: www.elsevier.com/locate/ejpb

Research paper

# Wavelength dependent photo-cytotoxicity to ovarian carcinoma cells using temoporfin loaded tetraether liposomes as efficient drug delivery system

Sajid Ali[a,b], Muhammad Umair Amin[a,b], Muhammad Yasir Ali[a,c], Imran Tariq[a,d], Shashank Reddy Pinnapireddy[a], Lili Duse[a], Nathalie Goergen[a], Christian Wölk[e,g], Gerd Hause[f], Jarmila Jedelská[a], Jens Schäfer[a], Udo Bakowsky[a,*]

[a] Department of Pharmaceutics and Biopharmaceutics, University of Marburg, 35037 Marburg, Germany
[b] Faculty of Pharmacy, The University of Lahore, 54000 Lahore, Pakistan
[c] Faculty of Pharmaceutical Sciences, GC University Faisalabad, Faisalabad, Pakistan
[d] Punjab University College of Pharmacy, University of the Punjab, 54000 Lahore, Pakistan
[e] Institute of Pharmacy, Martin Luther University Halle-Wittenberg, 06120 Halle, Germany
[f] Biocenter of the Martin-Luther-University Halle-Wittenberg, 06120 Halle, Germany
[g] Institute of Pharmacy, Pharmaceutical Technology, Faculty of Medicine, Leipzig University, 04317 Leipzig, Germany

ARTICLE INFO

*Keywords:*
Atomic force microscopy
Chorioallantoic membrane
Comet
Cryo-TEM
Hemocompatibility
Photodynamic therapy
ROS

ABSTRACT

5,10,15,20–Tetrakis(3–hydroxyphenyl)chlorin (mTHPC; temoporfin) is one of the most potent second-generation photosensitizers available today for the treatment of a variety of clinical disorders and has a unique capability of being activated at different wavelengths. However, due to its highly lipophilic nature, poor solubility in the aqueous media and poor bioavailability limits its application in anticancer therapies. To overcome these potential issues, we developed three different liposomal formulations with mTHPC encapsulated in hydrophobic milieu thus increasing the bioavailability of the drug. The prepared formulations were characterized in terms of hydrodynamic diameter, surface charge, encapsulation efficiency, and stability studies. The mean size of the liposomes was found to be in the nanoscale range (about 100 nm) with zeta potential ranging from −6.0 to −13.7 mV. mTHPC loaded liposomes were also evaluated for morphology using atomic force microscopy (AFM) and cryo-transmission electron microscopy (cryo-TEM). Data obtained from the hemocompatibility experiments showed that these formulations were compatible with blood showing less than 10% hemolysis and coagulation time lower than 40 s. The results obtained from the single-cell gel electrophoresis assay also demonstrated no incidence of genotoxicity. Photodynamic destruction of SK-OV-3 cells using mTHPC loaded liposomes showed a dose-response relationship upon irradiation with two different wavelength lights (blue λ = 457 nm & red λ = 652 nm). A 10-fold pronounced effect was produced when liposomal formulations were irradiated at 652 nm as compared to 457 nm. This was also evaluated by the quantitative assessment of reactive oxygen production (ROS) using fluorescence microscopy. The qualitative assessment of PDT pre- and post-irradiation was visualized using confocal laser scanning microscopy (CLSM) which demonstrated an intense localization of mTHPC liposomes in the perinuclear region. Chick chorioallantoic membrane assay (CAM) was used as an alternative *in-ovo* model to demonstrate the localized destruction of tumor microvasculature. Overall, the prepared nanoformulation is a biocompatible, efficient and well characterized delivery system for mTHPC for the safe and effective PDT.

## 1. Introduction

A tumor is a highly heterogeneous complex disorder characterized by uncontrolled and infinite growth of abnormal cells. They may perfuse the nearby tissues and other parts of the human body through dislocation into the blood and lymphatic system termed as metastasis, which is the primary cause of death from cancer. Currently used strategies for the treatment of cancer utilize the combination of chemotherapy, surgery, radiation and immunotherapy. These therapies have limited success when the malignant cells are restricted to the treatment area and are also associated with a lot of unwanted effects [1]. Unfortunately, despite a lot of research on cancer treatment

* Corresponding author.
*E-mail address:* ubakowsky@aol.com (U. Bakowsky).

https://doi.org/10.1016/j.ejpb.2020.03.008
Received 7 October 2019; Received in revised form 27 February 2020; Accepted 4 March 2020
Available online 06 March 2020

strategies, the long-term prospect for patients is still unclear, which calls for the innovative approaches and delivery systems that can deliver the drugs at the cancer cell selectively with reduced toxicity to surrounding tissues.

Photodynamic therapy (PDT) is a very simple and minimally-invasive therapeutic approach that is being widely used for the treatment of cancer. The principal of PDT is based on the combination of a light-sensitive molecule (photosensitizer), oxygen and light. After being administered, the photosensitizer compound can be preferentially localized into the tumor tissue. The tumor area is then illuminated by a light of specific wavelength to activate the drug molecule (photosensitization) [2]. The presence of tissue oxygen plays a key role in a successful PDT. After absorption of light energy of a particular wavelength, the photoactivated sensitizer interacts with molecular oxygen in the tissue to generate free radicals and singlet oxygen species. These highly ROS then oxidize the cellular and subcellular organelles to induce apoptosis or necrosis leading to tumor destruction. These species are very short-lived; therefore, the resultant tissue damage occurs very close to the production site.

The compound mTHPC (5,10,15,20–Tetrakis(3–hydroxyphenyl) chlorin) is one of the oldest yet most potent 2nd generation synthetic photosensitizers (PS) belonging to the family of chlorin photosensitizers. mTHPC requires lower activation energies to produce an efficient photodynamic effect. Being a chlorin compound, it is normally activated with red light at a longer wavelength of 652 nm and is indicated for the treatment of the different types of cancers i.e. head and neck carcinoma [3,4]. But due to its highly hydrophobic nature, it is poorly soluble in the biological medium such as blood plasma. In the aqueous environment, it tends to form aggregates and bind strongly to serum proteins, that limits its bioavailability which results in lower delivery, reduced tumor selectivity and lesser tumor uptake consequently reducing its photodynamic efficacy [5,6].

The incorporation of the poorly water-soluble PS in general is widely used and one option is the formulation with conventional diester phospholipids to form the liposomes. But the premature release of the PS into the bloodstream before reaching the tumor site, premature degradation of the liposomes due to the exchange between the phospholipids and lipoproteins and the opsonization of the conventional liposomes lead to the quick removal of the liposomes from the circulation. All these factors end up into reduced plasma half-life and consequently reduced PS accumulation in the tumor site. The liposomal size and lipid composition are also considered to be the important factors for the efficient delivery of the antitumor agents because these parameters play a critical role in the cellular uptake and their blood circulation time. The size dependence of the liposomes in the blood circulation can be attributed to their uptake by the mononuclear phagocytic system (MPS). Generally, a reduction in liposome size reduces its recognition by the complement system in the blood. It is believed that the size of about 100 nm is considered to be an optimal size for more efficient blood-tumor drug transfer and longer retention in tumor tissue [7].

To overcome the limiting stability of conventional diester phospholipids the use of natural ether lipids can be used. The plasma membrane of the archaea is rich in tetraether lipids (TELs) and diphytanylgylcerol diether also known as archeals [8]. Archaeal TELs are a mixture of caldarchaeol (glycerol dialkyl glycerol tetraether, GDGT) and calditoglycerocaldarchaeol (glycerol-dialkyl-nonitol tetraether, GDNT). GDGT consists of one glycerol backbone at each end of the hydrophobic core while GDNT contains one glycerol and calditol group at each end of the hydrophobic backbone. This hydrophobic core is composed of two phytanyl hydrocarbon chains ($C_{40}$) containing cyclopentane rings. As the number of cyclopentane rings is increased, it results in the tightening of the membrane packing. It is believed the presence of higher molar fractions of the TELs in the liposomal formulations results in the increased stability of the liposomal membrane.

The current study was aimed at the development of novel liposomal formulations encapsulating mTHPC to enhance the liposomal stability, prolonged circulation time and to compare the photodynamic effect in Ovarian carcinoma cells (SK-OV-3). The photodynamic effect was evaluated after activating the PS at different wavelengths. The prepared formulations were evaluated using Photon correlation spectroscopy (PCS) and Laser doppler velocimetry (LDV) for size distribution and surface charge respectively. Morphological studies were conducted using AFM and cryo-TEM. In addition, the chick CAM was conveniently used as an alternative *in-vivo* model to study the effect of prepared mTHPC-liposomes, and the photo-destruction of CAM microvasculature as well as the photothrombic effect was evaluated. *In-vitro* hemocompatibility for all the formulations was determined using activated partial thromboplastin time (aPTT) and *ex-vivo* hemolysis assay. Stability studies using simulated physiological conditions (in serum) were also conducted.

## 2. Materials and methods

### 2.1. Materials

mTHPC (5,10,15,20 Tetrakis(3 hydroxyphenyl)chlorin) was purchased from Cayman chemicals (Hamburg, Germany). 1,2-dipalmitoyl-*sn*-glycero-3-phosphatidylcholine (DPPC), 1,2–dipalmitoyl-*sn*-glycero-3-phosphoethanolamine-N- [methoxy (polyethylene glycol)-5000] (DPPE-$mPEG_{5000}$) were obtained as gift sample from Lipoid GmbH (Ludwigshafen, Germany). TELs were extracted from *Sulfolobus acidocaldarius* (TransMIT GmbH, Giessen, Germany). Tert-butyl hydroperoxide (TBHP), 2′,7′-dichlorodihydrofluorescein diacetate ($H_2$DCFDA) cholesterol and 3–(4.5-dimethylthiazol-2yl)-2,5-diphenyltetrazolium bromide (MTT) were obtained from Sigma Aldrich Chemie GmbH (Taufkirchen, Germany). Dimethyl sulfoxide (DMSO) was procured from Carl Roth GmbH & Co. (Karlsruhe, Germany). Iscove's modified medium (IMDM), Dulbecco's modified Eagle's minimum essential medium (DMEM), Fetal calf serum (FCS) were purchased from Capricon scientific (Ebsdorfergrund, Germany). Organic solvents (chloroform ($CHCl_3$), methanol (MeOH), ethanol (EtOH)) were obtained from VWR International (Pennsylvania, USA). Purified water (PureLab flex-2 dispenser, ELGA Lab water, High Wycombe, UK) was sterile filtered prior to use. Phosphate buffered saline (PBS) pH 7.4 (both with and without $Ca^{2+}$/$Mg^{2+}$) was freshly prepared, sterile and filtered in the laboratory for further use.

### 2.2. Preparation of mTHPC loaded liposomes

Liposomes were formulated using the traditional thin-film hydration method [9]. Briefly, three different lipid compositions: DPPC/Cholesterol $13.4 \times 10^{-3}$ M (90:10 M ratio), DPPC/DPPE–$mPEG_{5000}$ $6.9 \times 10^{-3}$ M (95:5 M ratio) and DPPC/TEL $4.3 \times 10^{-3}$ M (90:10 M ratio) were dissolved in organic solvent mixture (chloroform: methanol 2:1; v/v). The organic solvents were evaporated using a rotary evaporator (Heidolph Laborota 4000 efficient, Heidolph Instruments, Schwabach, Germany) equipped with a vacuum pump at 41 °C. For drug-loaded liposomes, mTHPC was added to the lipid mixture in a ratio of 1:20. The film was then re-hydrated using 1 mL of PBS (pH 7.4) and thoroughly agitated to form $7.35 \times 10^{-3}$ M mTHPC loaded liposomes. The pre-formed liposomes were then sonicated in a bath-type sonicator (Elmasonic P30H, Elma Schmidbauer, Singen, Germany) above the phase transition temperature ($T_g$) of the dominant lipid (i.e. DPPC = 41 °C) for 15 min. The obtained multilamellar liposomes (MLVs) were then extruded 21 times using polycarbonate membrane filters (Nuclepore track-etch membrane, Whatman GmbH, Germany) first through 200 nm and subsequently through 100 nm using Avanti mini-extruder® (Avanti Polar Lipids, Alabama, USA) to obtain unilamellar liposomes. The extruded liposomes were stored at 4 °C until further analysis [10].

### 2.3. Physicochemical characterizations

The hydrodynamic diameter of the liposomes was measured by PCS using Zetasizer Nano ZS (Malvern Panalytical GmbH, Kassel, Germany), equipped with a 10 mW HeNe laser at a wavelength of 633 nm at 25 °C and scattered light detection at 173°. Laser attenuation and measurement positions were automatically adjusted by the instrument with each measurement. The average particle diameter and polydispersity index (PDI) was always measured using disposable capillary cell (DTS1060, Malvern Instruments) for all the samples by diluting the liposomes (1:100) with purified water [12]. Data are expressed as mean ± standard deviation (SD) from the measurement of three independent samples (n = 3) with each measurement comprising of 15 individual runs. All the results were expressed as the size distribution by intensity.

The zeta potential (ζ) of mTHPC loaded liposomes was performed with Zetasizer Nano ZS by measuring the electrophoretic mobility with LDV at 25 °C and a scattering angle collection at 17°. A clear disposable folded capillary cell (DTS1060) was used for this purpose. Prior to measurement, the samples were subsequently diluted as described above. The values are expressed as mean ± SD for the measurement of three independent samples. Three individual samples were measured for this purpose with every measurement having 15–100 runs, depending on the sample [13].

### 2.4. Encapsulation efficiency

The encapsulation efficiency (EE%) of mTHPC loaded liposomes was determined by the solvent extraction technique using air-driven ultracentrifuge Airfuge® (Beckman Coulter GmbH, Krefeld, Germany). Briefly, 200 µl of prepared liposomes were centrifuged for 90 min at 20 PSIG (60,000 rcf) using Beckman Polyallomer microcentrifuge tubes (Beckman Coulter GmbH, Krefeld, Germany). After centrifugation, the supernatant was separated and the pellet was resuspended using 200 µl of ethanol. Similarly, an equal amount of ethanol was added to the supernatant. Further centrifugation steps were carried out to remove and discard any undissolved lipids. The amount of mTHPC encapsulated was quantified from both solutions using Multiskan™ GO UV/VIS microplate spectrophotometer (Thermo Fischer Scientific GmbH, Dreieich, Germany). Liposomes having the same lipid composition without mTHPC were used as a blank. The calibration curve for mTHPC was constructed in both ethanol and ethanol/water (1:1). The EE% was determined using the following formula [14]:

$$EE\% = \frac{\text{Amount of drug encapsulated}}{\text{Total amount of drug added}} \times 100 \quad (1)$$

### 2.5. Morphological characterizations using AFM:

A total of 50 µl of diluted sample dispersion (1:100 with purified water) was transferred to the silicon chip mounted on the glass slide and left to settle down for 15 min. The supernatant was then removed by aspiration using a tissue (KIMTECH Science, Kimberly-Clark Europe Limited) and the sample was allowed to dry. AFM was performed using vibration damped (i4 Series - Active Vibration Isolation, Accurion GmbH, Göttingen, Germany) NanoWizard®-3 NanoScience AFM system (JPK BioAFM, Bruker Nano GmbH, Berlin, Germany). Commercially available soft n-type silicon 1-lever cantilever tips (HQ: NSC14/AL_BS, Mikromasch Europe, Wetzlar, Germany) with a resonance frequency of 160 KHz and nominal force constant of 5 N/m were used for the measurements. The scan speed was adjusted between 0.5 and 1.5 Hz. These measurements were performed using the intermittent contact mode in the air to avoid the liposome's disruption. The images were visualized using height measured mode. The raw images were processed with JPK data processing software [15,16].

### 2.6. Cryo-TEM analysis

Cryo-TEM was performed as described by Janich et al. [17]. The vitrified liposomal samples were examined using the blotting technique. The process was performed at room temperature in a humidity-controlled environmental chamber of an EM GP grid plunger (Leica Microsystems, Wetzlar, Germany). Briefly, 6 µl of the sample was placed on a grid coated with an ultra-flat holey carbon film (C-flat, Protochips Inc., Raleigh, NC). The excess liquid was removed by blotting using a filter paper. The grids were plunge-frozen immediately by immersing in liquid ethane and maintained at a temperature below 108 K (−165.15 °C). The frozen grids were transferred into a Libra 120 transmission electron microscope (Carl Zeiss Microscopy GmbH, Jena, Germany; acceleration voltage 120 kV) equipped with a Gatan 626 cryotransfer system. Images were taken with a BM-2k-120 dual-speed on-axis SSCCD camera (TRS, Moorenweis, Germany) [17].

### 2.7. Cell line and culturing

SK-OV-3 cells were procured from ATCC (American type culture collection, Manassas, USA). The cells were cultivated at 37 °C and 7% $CO_2$ under humid conditions in a high glucose DMEM supplemented with 10% FCS and MEM-non-essential amino-acids (Gibco™, ThermoFischer). The cells were grown as a monolayer and passaged to confluency [9,14].

### 2.8. Light delivery to the cells

A prototype LED device containing light-emitting diodes (Generation-I LED irradiator, Lumundus GmbH, Eisenach, Germany) was used. The device was equipped with the function to change the irradiation time (s) and current (mA) as required. It was supplied with two different LEDs of 457 nm (blue) and 652 nm (red) wavelengths. The device was able to deliver irradiance of 22.4 $Wm^{-2}$ at a current of 20 mA and wavelength of 652 nm. Similarly, 220.2 $W/m^2$ irradiance can be delivered at a current of 100 mA and a wavelength of 457 nm. The actual light dose ($Jcm^{-2}$) delivered to the cells seeded in 96 well plates is equal to irradiance ($Wcm^{-2}$) times the irradiation time.

### 2.9. Cellular photodynamic therapy (cPDT)

The cells were seeded in the clear flat bottom 96 well microtiter plates (Nunclon Delta, Thermo Fischer Scientific GmbH, Dreieich, Germany) at a seeding density of 10,000 cells/well (0.35 $cm^2$). Post 24 h stabilization, the cells were incubated with mTHPC loaded liposomes in different concentrations ranging from 5 µM to 0.05 µM (appropriately diluted with the medium). The incubation time was set to 2 h after initial incubation for different times e.g. 1 h, 2 h, and 4 h. After the incubation, the liposomal formulations were replaced with fresh medium and the mTHPC taken up by the cells was irradiated at 652 nm (red) for 23, 223 and 446 s at a fluence of 22.4 $Wm^{-2}$ (20 mA). This corresponds to 0.05, 0.5 and 1 $Jcm^{-2}$ of the total light dose delivered respectively. Similarly, in other experiments, mTHPC was illuminated at 457 nm (blue) for 45, 227 and 455 s at a fluence of 220.2 $W/m^2$ (100 mA) which corresponds to 1, 5 and 10 $Jcm^{-2}$ of total light energy delivered. An unirradiated well plate treated in the same way with liposomal formulations was considered as dark control. After 24 h, the medium was replaced with the MTT reagent appropriately diluted with medium (2 mg/mL) and incubated for 4 h. After the incubation, medium containing MTT dye was aspirated and formazan crystals were dissolved using DMSO. Free mTHPC in the same concentration dissolved in DMSO due to its low solubility in water was taken as a standard control whereas cells, without any liposomal formulation were considered as a negative control. The absorbance was recorded at 570 nm using FLUOStar Optima plate reader (BMG Labtech, Ortenberg, Germany). The cell viability of the untreated cells was considered to be

100%. The cell viability of treated cells was calculated as [9]:

$$\text{Cell Viability } \% = \frac{Ab_{Sample} - Ab_{Blank}}{Ab_{Control} - Ab_{Blank}} \times 100 \quad (2)$$

where $Ab_{Sample}$ and $Ab_{Control}$ denote the treated and untreated samples respectively. While $Ab_{Blank}$ indicates the well containing medium without any cells. The values are expressed as mean ± SD with all the experiments performed in triplicate.

### 2.10. Intracellular uptake studies

For intracellular uptake analysis of mTHPC encapsulated liposomes, SK-OV-3 cells were seeded onto the sterile cover glasses (15 × 15 mm) placed in 12 well cell culture plates (Nunclon Delta, Nunc GmbH & Co. KG., Wiesbaden, Germany) at a density of 90,000 cells/well. After 24 h, the medium was replaced by 5 μM of mTHPC loaded liposomes and incubated for 2 h at 37 °C. After the incubation, the medium was aspirated and cells were washed twice with sterile ice-cold PBS (pH 7.4) supplemented with $Ca^{2+}$ & $Mg^{2+}$. The cells were then fixed with 4% formaldehyde by incubating the cells for 20 min at room temperature. They were then washed again with PBS (pH 7.4). The cell nuclei were counterstained with 50 nM of Sytox green™ nucleic acid stain (ThermoFischer Scientific GmbH, Dreieich, Germany) for 20 min. After washing twice with PBS (pH 7.4), the cover glasses were then removed from the well plate, mounted on glass slides and sealed with fluorescence free glycerol-based FluorSave™ reagent (Calbiochem, San Diego, USA). The stained cells were then observed under the LSM700 confocal laser-scanning microscope (Carl Zeiss Microscopy, Jena, Germany). The cellular uptake was then observed using fluorescence detection filters for Sytox green™ ($\lambda_{ex/em}$ 504/523 nm) and mTHPC ($\lambda_{ex/em}$ 420/652 nm) [18,19].

### 2.11. Measurement of cellular reactive oxygen species (cROS)

The quantitative determination of ROS was performed using a free radical sensor and cell-permeable fluorescent dye $H_2$DCFDA. The assay was performed according to the DCFDA cellular ROS detection protocol from Abcam with slight modifications. Briefly, SK-OV-3 cells were seeded in the dark, clear bottom 96 well microtiter plates at a density of 25,000 cells/well. Cells were allowed to adhere overnight. On the following day, the cells were washed with PBS (pH 7.4) supplemented with $Ca^{2+}$ and $Mg^{2+}$ and were then incubated with 25 μM of $H_2$DCFDA, by incubation for 45 min at 37 °C. After washing again with PBS, they were incubated with mTHPC loaded liposomes for 2 h. 50 μM of TBHP was used as a positive control. After the incubation, cells were irradiated at a radiation fluence of 1 $Jcm^{-2}$ at 457 and 652 nm. The cells were then washed with PBS and the fluorescence was recorded at $\lambda_{ex}$ 480 nm/$\lambda_{em}$ 520 nm using FLUOStar Optima plate reader. Based on the results obtained from cPDT and measurement of cROS, the irradiation was done using 652 nm wavelength light for the further experiments [19].

### 2.12. Ex-vivo hemolysis assay

To evaluate the effect of mTHPC loaded liposomes on human blood, the *ex-vivo* hemolysis assay was performed as described by Raschpichler et al. [20]. Briefly, 10 mL of fresh human blood was drawn into the EDTA tubes to prevent the coagulation and centrifuged at 500*g* for 5 min, resulting in separation of blood plasma from the human erythrocytes. The plasma was aspirated and erythrocyte pellet was washed three times with sterile PBS (pH 7.4) and diluted to 1:50 with PBS. mTHPC loaded liposomes (10X of the desired final concentration tested in cell culture experiments) were then incubated with erythrocytes in V-bottom microtiter plates for 1 h at 37 °C in an orbital shaker KS4000 IC (IKA Werke, Staufen, Germany). The plates were then centrifuged and the supernatant was transferred into a clear flat bottom 96 well plate. The absorbance was measured at 540 nm using FLUOStar Optima plate reader. Sterile filtered PBS (pH 7.4) and 1% Triton™ X-100 were taken as negative and positive controls, respectively. The absorbance value from Triton™ X-100 was considered as 100% hemolysis. The assay was done in triplicate and the results were expressed as mean ± SD [20].

### 2.13. aPTT test

In order to verify that the mTHPC loaded liposomes do not trigger the coagulation cascade upon intravenous administration, aPTT test was performed as described by Pinnapireddy et al. [21]. The test was performed in the Coatron M1 coagulation analyzer (TECO GmbH, Neufahrn, Germany) using TEClot aPTT-S kit as described by the manufacturer's manual with slight modifications. Briefly, fresh blood was drawn in a citrate tube and centrifuged at 1500*g* for 15 min to separate the blood plasma. 25 μl of the plasma was mixed with 25 μl of the sample, followed by the addition of 50 μl of aPTT reagent for the activation of coagulation factors. Finally, 0.025 M prewarm calcium chloride ($CaCl_2$) was added to the mixture to activate the coagulation of blood. Coagulation was confirmed spectrophotometrically, and the clotting time was recorded in seconds. The experiments were performed in triplicate and the results were expressed as mean ± SD [21].

### 2.14. Photo-thrombic activity of mTHPC liposomes

Fertilized eggs weighing 50–60 g were purchased from Mastkükenbrüterei Brormann (Rheda-Wiedenbruck, Germany). After the delivery, the eggs were disinfected with ethanol (70%) and placed in a hatching incubator (Dipl. Ing. W. Ehret GmbH, Emmendingen, Germany) equipped with the automatic rotator at a temperature of 37 °C and relative humidity of 65%. This day was considered as egg development day 0. The intact chick CAM angiogenesis model was used as described by Tariq et al. [22], with slight modifications. Briefly, on EDD 4 a 30 mm hole was made on the apical part of the egg with the help of pneumatic egg puncher (Schuett Biotech GmbH, Germany) at a pressure of about 2–3 bars to expose the premature CAM surface. The exposed surface was then covered with a small petri dish and placed back to the incubator in the static upright position until the CAM was fully developed. On EDD 12, 100 μl of the liposomal sample (200 μM) was injected intravenously *in-ovo* using a stereo-microscope (Stemi 2000-C, Carl Zeiss GmbH, Jena, Germany) and incubated for 60 min. After the homogenous distribution of the sample, a PVC ring (diameter 5 mm) was placed on a predefined treatment area. An image of the CAM surface was recorded prior to irradiation. Subsequently, the chosen area was irradiated using a red laser diode (652 nm, 40 mW) with Weber needle catheters (Weber Medical GmbH, Lauenförde, Germany). The irradiation was performed for 2 min at an area of 3.1 $mm^2$ that corresponds to 4.8 $Jcm^{-2}$ energy (optimized energy; data not shown). Vascular occlusion was recorded post-irradiation from 10 min to 48 h using Stemi 2000-C stereo-microscope (Carl Zeiss GmbH, Jena, Germany) attached with a Moticam 5 CMOS camera (Motic Deutschland GmbH, Wetzlar, Germany). For each liposomal formulation, the experiment was performed in triplicate and images were recorded pre and post photodynamic treatment. Eggs treated with normal saline were considered as a negative control [23,24].

### 2.15. Serum protein interactions with liposomes

The serum induced changes in size of mTHPC encapsulated liposomes were evaluated in simulated conditions. In order to simulate the physiological conditions, 0.2 mL mTHPC loaded liposomes were mixed with 1 mL of 60% FCS (diluted in PBS (pH 7.4) to get a volume ratio of 5. Similarly, 1 mL PBS (pH 7.4) was also mixed with 0.2 mL of mTHPC containing liposomes to get the same volume ratio of 5. Both of the mixtures were then incubated for 24 h in a shaking incubator at

100 rpm and 37 °C. In the control experiments, only PBS (pH 7.4) was mixed with FCS keeping the other parameters constant. The samples were withdrawn at specific time intervals, appropriately diluted with purified water and measured using Zetasizer Nano ZS. The results were obtained for three independent formulations [25].

### 2.16. Single cell gel electrophoresis

The single-cell gel electrophoresis (Alkaline Comet Assay) was used to assess the DNA damage and genotoxicity induced by mTHPC encapsulated liposomes. All the procedures were performed in dark [26]. Briefly, 1,00,000 SK-OV-3 cells per well were seeded into a six-well plate and were allowed to adhere overnight. The following day the cells were incubated with 0.5 μM of mTHPC loaded liposomes for 2 h. After the incubation is over, the mTHPC liposomes were replaced with the fresh medium. Consequently, the cells were irradiated at an equitoxic light dose to produce 80% cell viability in order to avoid any false positive responses. The treated cells were then incubated overnight. The next day, the cells were trypsinized and centrifuged for 5 min at 1000 rpm to get the cell pellet. The obtained cell suspension was washed twice using sterile PBS (pH 7.4) and cell density was adjusted accordingly. As a next step, 80,000 cells (25 μl) of the PDT treated cell suspension was mixed with 75 μl of 1% of prewarm low melting agarose (LMA) (Carl Roth GmbH, Karlsruhe, Germany). The mixture was applied on the superfrost glass slide previously precoated with of 1% standard normal melting agarose (NMA) and was immediately covered with coverslips. The glass slides were then placed on an ice block for 10 min until solidified and the coverslips were gently removed. The cell membrane lysis was done by submerging the slides overnight into the staining jar containing cold lysis solution (300 mM NaOH, 1.2 M NaCl, 2% DMSO and 1% Triton™ X-100) [27]. The slides were then transferred to the electrophoresis tank containing alkaline electrophoresis buffer (300 mM NaOH and 1 mM EDTA) and were left in the buffer for 30 min to allow the unwinding of DNA. Electrophoresis was performed for 30 min at 250 mA current and 25 V, resulting in the DNA unwinding and exposing the alkali labile sites. After the electrophoresis, the slides were neutralized by washing the slides with double distilled water. The cell fixation was then done by submerging the slides into the 70% ethanol for 20 min. After fixation, the slides were cells were stained with SYBR® safe DNA staining dye (1:10,000 in PBS) for 20 min. Finally, the slides were washed with double distilled water to remove any unbound stains. The comet analysis was done under a fluorescence microscope (CKX-53 Olympus, USA). Fifty individual comets were scored for each formulation.

### 2.17. Cellular uptake pathway analysis

In order to determine the liposomal uptake mechanism by the cells, the SK-OV-3 cells were seeded into a 96 well plate at a seeding density of 10,000 cells/well and were allowed to adhere overnight by maintaining at 37 °C and 5% $CO_2$. The next day, the cells were washed with PBS (pH 7.4) supplemented with $Ca^{2+}/Mg^{2+}$. The cells were then pre-incubated with the inhibitors of the vesicular uptake pathway (i.e. Chlorpromazine 30 μM and Filipin-III 15 μM) for 1 h. After incubation is over, mTHPC loaded liposomes were added to the cells at a concentration of 1.5 μM and were again incubated for a total time of 3 h. Post incubation, the liposomes were replaced by fresh medium and irradiation was performed at a light dose of 1 $Jcm^{-2}$. Subsequently, the cells were incubated again for 24 h. Un-irradiated plates were taken as the dark control. The following day, cell viability was determined using MTT assay as described previously [10].

### 2.18. Statistical analysis

Non-linear curve fitting functions were applied on normalized dose-response cell viability data obtained from photodynamic MTT assays and $IC_{50}$ values were calculated. All the experiments were performed in triplicate unless otherwise stated and results are expressed as mean ± SD. Two-way analysis of variance (ANOVA) with Dunnett's test (multiple comparisons against a control group) was performed for the comparison of percentage viability obtained from cytotoxicity assays. One-way ANOVA with post hoc test (Dunnett's multiple comparisons against control) was performed on data obtained from hemolysis and comet assay using Graph Pad Prism 5. Significance levels of $p < 0.05$ were considered for the rejection of the nulls hypothesis.

## 3. Results and discussion

### 3.1. Physicochemical properties of liposomes

Liposomal formulations not only facilitate the administration of the hydrophobic PS but also avoid their precipitation into the aggregated form which results in increased bioavailability with higher accumulation of PS at the tumor site [28]. By assimilating the PS into the liposome, the fluidity of the system can be altered and hence delivery process of the photosensitizer can be modified. mTHPC being a hydrophobic molecule, tend to align itself in the non-polar region of the liposomal bilayer membrane where it contributes to strong hydrogen-bonding interactions with the polar heads of the phospholipids (e.g. DPPC). mTHPC acts as a hydrogen donor because of the strong electron-withdrawing effect of the aromatic ring of its phenolic constituents [29]. This drug-lipid interaction can lower the molecular motion of phospholipids giving rise to more rigid and stable systems. These interactions are also responsible for higher loading capacity and reduced fluidity of the membrane [30,31]. In the current study, three different liposomal formulations were used to study their effect on cellular uptake, serum stability, biocompatibility, and light-induced toxicity. The composition of prepared liposomes and their physicochemical properties are presented in Table 1. All the prepared liposomal formulations contained DPPC as major vesicle-forming lipid combined with other lipids in specified molar fractions. No significant modification of liposomal size and zeta potential was induced owing to the presence of different DPPC molar ratios in different liposome formulations. The hydrodynamic diameter of all the formulations was in nanometric range, ranging from 106.0 ± 5.5 nm to 129.2 ± 3.3 nm with a PDI of less than 0.2 for the formulation containing DPPC/Cholesterol, which represents the narrow monomodal distribution of liposomal vesicles. The liposome containing TEL and DPPE-$mPEG_{5000}$ in small molar

**Table 1**
Physicochemical properties of mTHPC loaded liposomes. Each liposome consists of 5% of mTHPC (m/total lipid%). Hydrodynamic diameter is expressed as a function of particle size distribution by intensity. Values are expressed as mean ± SD for three independent measurements (n = 3).

| Formulation (mol%) | Diameter (nm) ± SD | PDI ± SD | Surface Charge (mV) ± SD |
|---|---|---|---|
| DPPC: Cholesterol (90:10) | 106.00 ± 5.50 | 0.17 ± 0.02 | −9.45 ± 2.58 |
| DPPC: DPPE-$mPEG_{5000}$ (95:5) | 117.80 ± 8.12 | 0.20 ± 0.03 | −9.59 ± 1.86 |
| DPPC: TEL (90:10) | 111.00 ± 1.30 | 0.27 ± 0.03 | −15.50 ± 3.55 |
| DPPC: Cholesterol (90:10)-mTHPC | 109.60 ± 2.20 | 0.13 ± 0.03 | −6.68 ± 0.39 |
| DPPC: DPPE-$mPEG_{5000}$ (95:5)-mTHPC | 129.40 ± 9.60 | 0.25 ± 0.03 | −8.98 ± 2.00 |
| DPPC: TEL (90:10)-mTHPC | 120.20 ± 3.31 | 0.23 ± 0.02 | −13.20 ± 2.09 |

**Table 2**
The encapsulation efficiency of mTHPC loaded liposomes (0.5 mg of mTHPC per 10 mg of total lipid). Values are expressed as mean ± SD for three independent formulations (n = 3).

| Formulation (mol%) | Theoretical drug load (μg/mL) | Practical drug load (μg/mL) ± SD | % EE ± SD |
|---|---|---|---|
| DPPC: Cholesterol (90:10)-mTHPC | 500.00 | 390.49 ± 20.02 | 78.09 ± 4.00 |
| DPPC: DPPE-mPEG$_{5000}$ (95:5)-mTHPC | 500.00 | 408.54 ± 14.84 | 81.70 ± 3.26 |
| DPPC: TEL (90:10)-mTHPC | 500.00 | 452.01 ± 19.05 | 90.40 ± 2.60 |

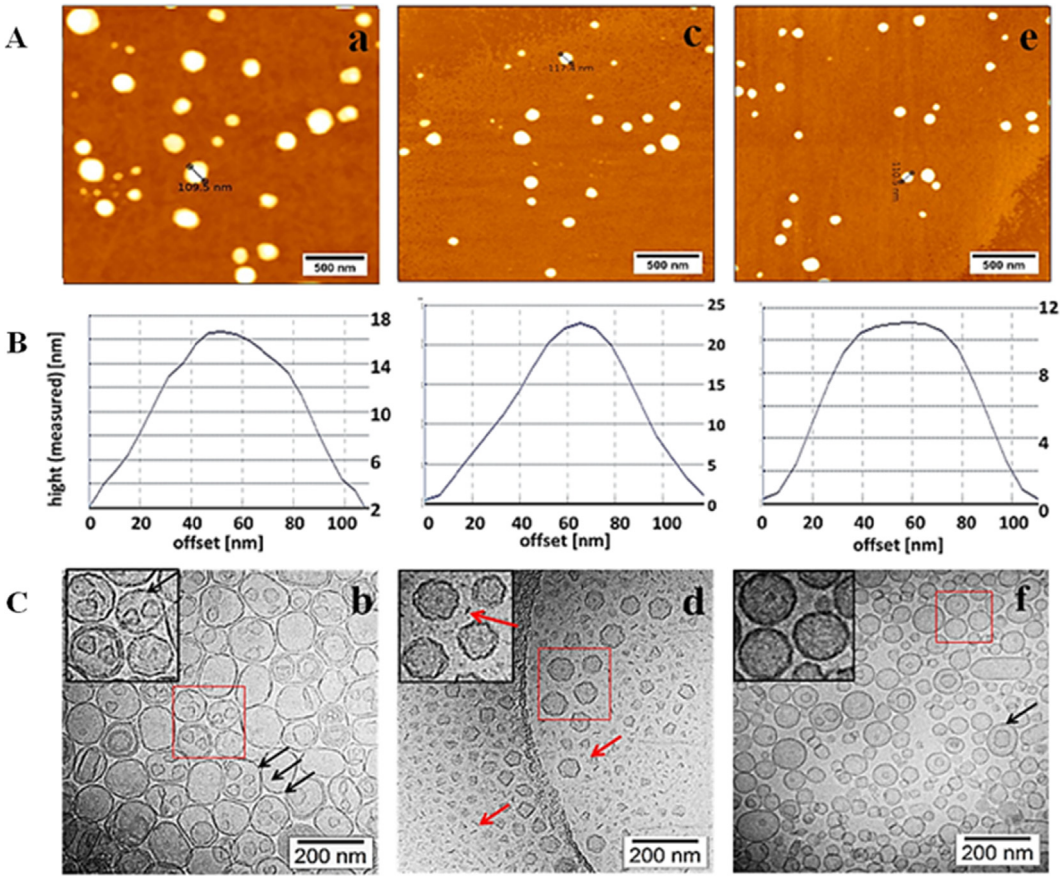


**Fig. 1.** AFM micrographs (1st Row) and Cryo-TEM images (3rd Row) showing the structural characteristics of mTHPC loaded liposomes. (a and b) DPPC/Cholesterol (c and d) DPPC/DPPE-mPEG$_{5000}$ and (e and f) DPPC/TEL. For AFM studies, soft HQ: NSC14/AL_BS cantilevers were used to obtain the height measured images in trace direction. Middle pane (2nd Row) showing the cross-sectional profile of the liposomes along the identified lines. The scale bar represents 500 nm for AFM images and 200 nm for Cryo-TEM images.

fractions exhibited a PDI of more than 0.2. This relatively higher PDI can be attributed to the presence of smaller disc-shaped liposomes and large PEG chains present in a formulation that also gives a stealth effect to the liposome [32]. All the liposomal formulation possessed an overall negative zeta potential ranging from −13.2 ± 2.0 to −6.6 ± 0.3 mV.

### 3.2. Encapsulation efficiency (EE%)

The encapsulation efficiency of mTHPC loaded liposomes was determined using the ultracentrifugation method. The results of mTHPC encapsulation in the lipid bilayer (Table 2) showed that more than 75% of mTHPC was encapsulated in all the liposomal formulations. DPPC/Cholesterol (90:10) liposomes showed the least amount of drug encapsulated i.e. 78.0 ± 4% which increased to highest in DPPC:TEL liposomes with an encapsulation efficiency of 90.40 ± 2.60%. This comparative higher encapsulation can be attributed to the fact that the liposomes made from the polar lipid fractions of *S. acidocaldarius* show a remarkable stability. This stability of the liposomes is due to the ability of TEL to preserve membrane integrity due to tight membrane packing that results in retaining the entrapped molecules with a very low leakage problem [23]. The overall high drug load in all the liposomes can be credited to the hydrophobic and intermolecular interactions (hydrogen bonding) between drug and lipid molecules [31].

### 3.3. Morphological characterizations using AFM and Cryo-TEM

Morphological interpretations of the mTHPC loaded liposomes were conducted using AFM and Cryo-TEM studies. For AFM studies, the images were acquired using intermittent contact mode. This intermittent tapping of the cantilever tip reduces the shear forces applied on liposomes, which can deform or burst the vesicle. Depending on the vesicle composition, interactions between the sample and substrate surface (e.g. glass or silicon), as well as the continuous oscillation of the tip, can induce the deformation of vesicles. Longer sample deposition times on the substrate may also lead to the formation of planner vesicles [33]. In our AFM studies, the liposomes appeared to be round or slightly oval-shaped. The diameter of the particles resulting from the analysis of the AFM micrographs was found to be in good correlation

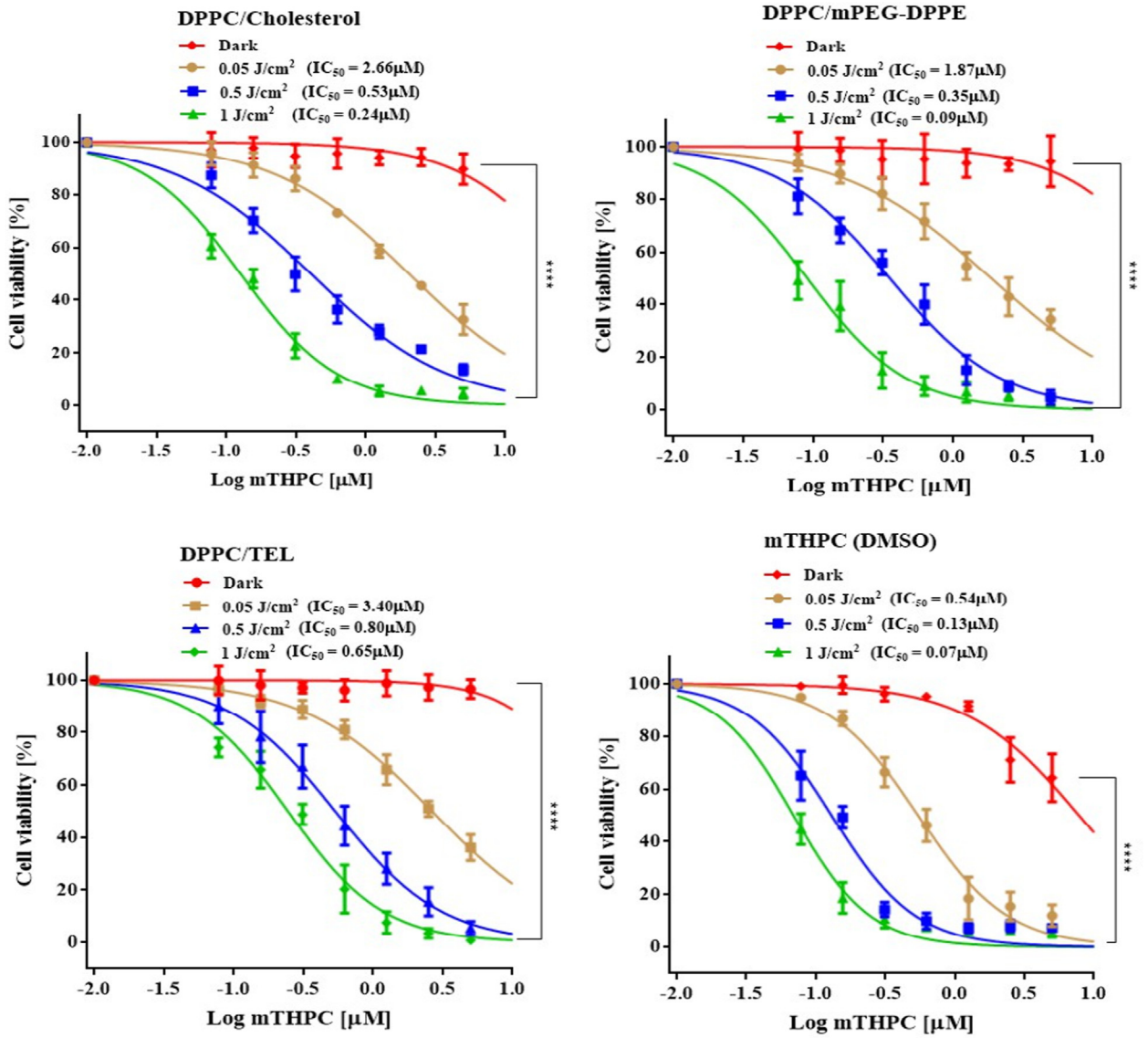


**Fig. 2.** Dose-response nonlinear curves representing photo-induced cytotoxicity (λ = 652 nm) to SK-OV-3 carcinoma cells. mTHPC formulations i.e. DPPC/Cholesterol, DPPC/DPPE-mPEG$_{5000}$, DPPC/TEL and free mTHPC dissolved in 0.1% DMSO were incubated for 2 h and then irradiated with series of light exposures of 0.05, 0.5 or 1 Jcm$^{-2}$ with red light. Whereas dark represents the formulations without irradiation. The half-maximal inhibitory concentration (IC$_{50}$) was calculated by non-linear curve fitting. Each value is represented as the mean ± SD for three independent experiments. For the statistical analysis, the comparison was done against the dark treatment. P values ($p < 0.05$) were considered significant and denoted as '****' ($p < 0.0001$) and '**' ($p < 0.01$). (For interpretation of the references to colour in this figure legend, the reader is referred to the web version of this article.)

with the hydrodynamic diameter obtained from PCS measurements (Table 1). The height measured view was used to analyze the liposomal size distribution parameters (Fig. 1). Some irregularly shaped liposomes also spread on the silicon surface like a sheet of lipid monolayer that might be due to the liposomal disruption during the preparation of samples [15].

Cryo-TEM is a significant tool for the visualization of delicate ultrastructure of colloidal drug delivery systems (e.g. liposomes). It is the most widely used technique to study the shape, size and the overall composition of these carrier systems as it permits the evaluation of colloidal dispersions in the vitrified frozen state. It has an advantage that the rapid cooling of samples ensures minimum perturbation of the original samples [34]. Fig. 1b, d, f, represents the typical cryo-TEM micrographs of mTHPC loaded liposomes. Preparation of liposomes by extrusion resulted in the population of mainly unilamellar vesicles but some fractions of bi- and oligolamellar vesicles, as well as multivesicular systems (black arrows in Fig. 1b and f), can also be observed. Liposomal formulation composed of DPPC/Cholesterol (90:10) has predominately shown the round and slightly elliptical structures (Fig. 1b). According to Almgren et al [34] the presence of cholesterol as well as the tight packing of the vesicles, under the influence of which, the liposomes tend to appear oval-shaped. For the formulations containing DPPE-mPEG$_{5000}$ in small molar fractions, disc-like associates (i.e. lipodisks) can be assumed along with other vesicular structures (red arrows, Fig. 1d). Kuntsche et al. [35] have found out that these discs appeared as small rods or thread-like in shapes (Fig. 1d) and can be credited to the presence of PEG chains in the formulation. When the concentration of the PEG grafted lipid reaches a limiting concentration, it becomes energetically more favorable to form a lipid/ lipid-polymer aggregates than bilayers. These aggregates may exist as a transition before the formation of micelles. Additionally, the absence of the cholesterol in the formulation also promote the formation of thread like structures even at a lower PEG-PE concentration. Nevertheless, the presence of discs needs more proof, because from the orientational

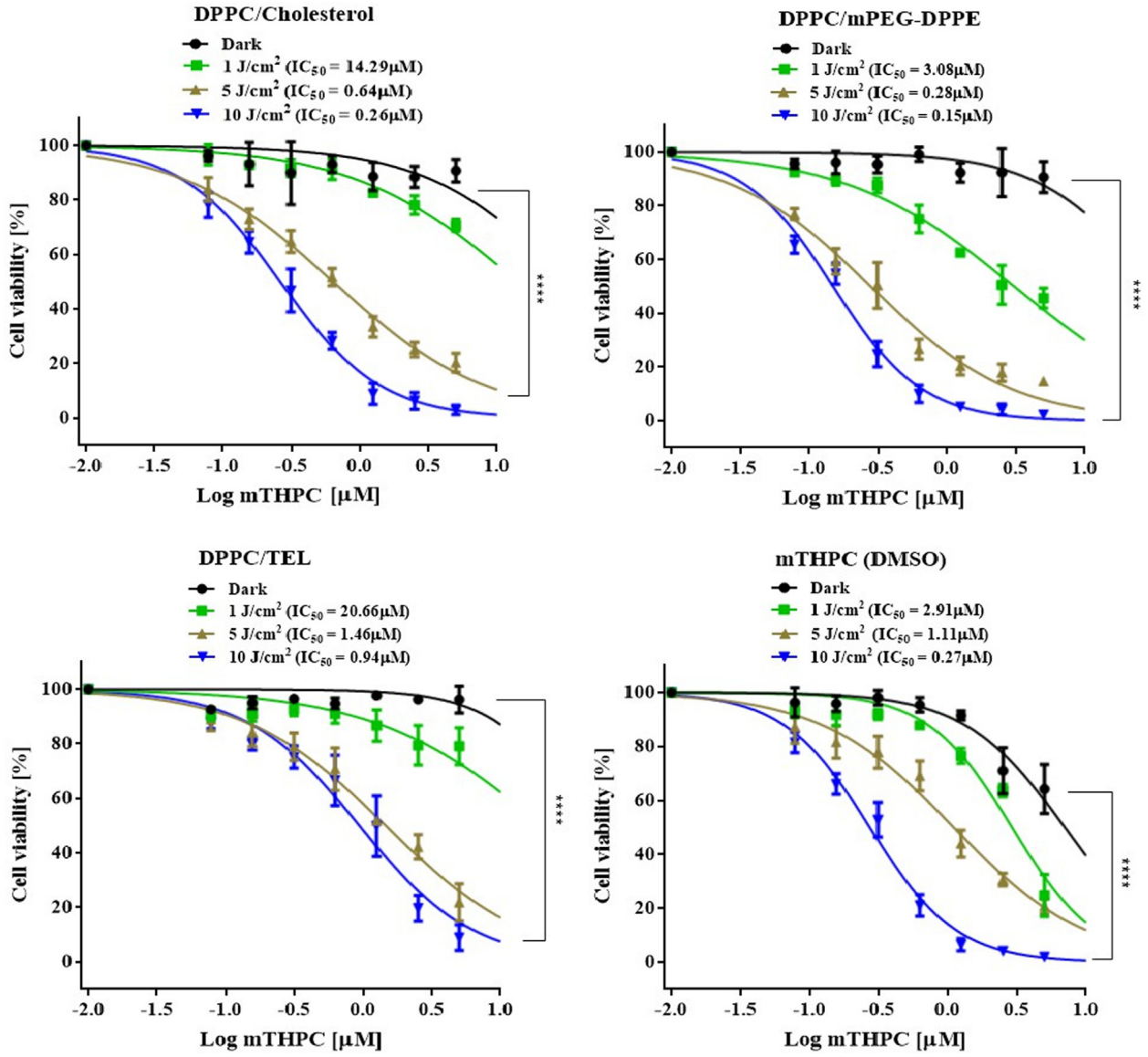


**Fig. 3.** Dose-response nonlinear curves representing photo-induced cytotoxicity (λ = 457 nm) to SK-OV-3 carcinoma cells. mTHPC formulations. i.e. DPPC/Cholesterol, DPPC/DPPE-mPEG$_{5000}$, DPPC/TEL and free mTHPC dissolved in 0.1% DMSO (D) were incubated for 2 h and then irradiated with series of light exposures of 1 Jcm$^{-2}$, 5 Jcm$^{-2}$ or 10 Jcm$^{-2}$ with blue light. Whereas dark represents the formulations without irradiation. The half-maximal inhibitory concentration (IC$_{50}$) was calculated by non-linear curve fitting. Each value is represented as the mean ± SD for three independent experiments. For the statistical analysis, the comparison was done against the dark treatment. P values ($p < 0.05$) were considered significant and denoted as '****' ($p < 0.0001$) and '**' ($p < 0.01$). (For interpretation of the references to colour in this figure legend, the reader is referred to the web version of this article.)

point of view they should also appear as circular structures and ellipses. In tetraether lipid-based formulation, liposomes also appeared circular or somewhat elongated (Fig. 1f). This is because of the rigidity of the lipid bilayer that may influence the liposome shape, as the TEL liposomes with a rigid membrane have the ability to preserve the membrane integrity by tight membrane packing of lipid molecules.

### 3.4. Cellular photodynamic therapy (cPDT)

The photo-destruction effect of mTHPC (free as well as liposome loaded) was investigated in the SK-OV-3 by assessing the percentage cell viability using MTT assay. It was carried out in the presence of different concentrations of mTHPC liposomes for 2 h in the dark followed by subsequent irradiation of the cells with a prototype LED Lamp with red light (λ = 652 nm). The initial 1 h incubation did not show any significant effect on the cell viability (data not shown), indicated the need for increased incubation time. The survival of SK-OV-3 cells, incubated with different mTHPC concentrations and irradiated with varying light fluences are represented in Fig. 2. Treatment of the cells with mTHPC (dissolved in 0.1% DMSO in medium) without subsequent irradiation resulted in a dose-dependent reduction of cell viability inferred as "dark toxicity". This dark toxicity was evident at the mTHPC concentration equal to or above 2.5 μM (1.7 μg/mL) (Fig. 2D) a can be assumed due to the presence of DMSO. In contrast, mTHPC encapsulated in liposomal formulations did not show any dark toxicity. These findings were in good correlation with the previous studies conducted by Reidy et al. [36]. At the light dose of 0.05 Jcm$^{-2}$, the cell viability was reduced to less than 40% in the treated groups (except for DPPC/TEL liposome) as compared to untreated controls. The cell viability in the untreated control group, without any formulation or mTHPC, remained of 95–98% which confirmed that the application of irradiation only, did not produce any significant cell destruction. For the formulation containing tetraether lipids, the cell viability was still recorded at about 60%. This could be due to the slower release of PS

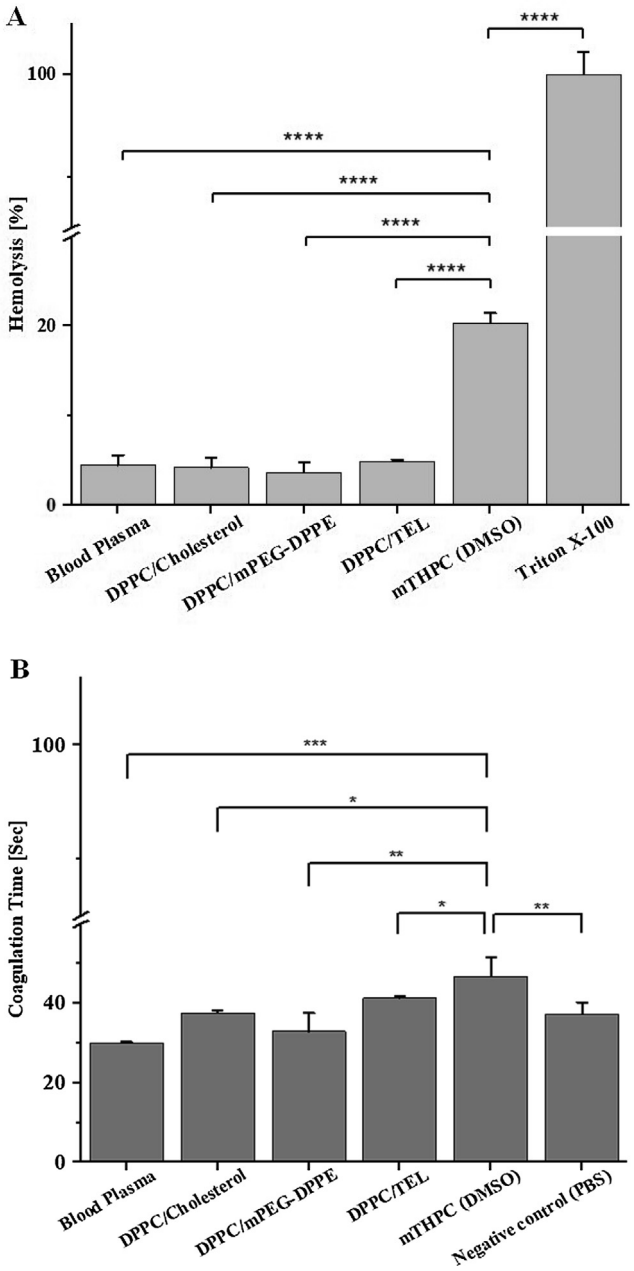


**Fig. 4.** Hemocompatibility assay; (A) Hemolysis assay & (B) aPTT test of mTHPC loaded liposomes. All the formulations were tested at 10× concentrations. Blood plasma and Triton X–100 were used as negative or positive control respectively. All the samples were measured in triplicate and the values were expressed as mean ± SD (n = 3). For the statistical analysis, the comparison was done against the free drug. P values ($p < 0.05$) were considered significant and denoted as '****' ($p < 0.0001$) and '**' ($p < 0.01$).

from the liposomal membrane, stabilized in the presence of tetraether lipids [23]. With increasing fluence, the cell viability continuously decreased in all the formulations, ending up at 18–20% at 1 $Jcm^{-2}$. Kiesslich et al. [38] obtained similar dose-response curves of 0.6 μM mTHPC with 20 h incubation time and fluences of 0.7–2.31 $Jcm^{-2}$. In our experiments when the fluence was kept constant and the concentration of mTHPC was varied between 0.05 and 5 μM, the half-maximal inhibitory concentration ($IC_{50}$) of the liposomes was also reduced proportionally. The highest reduction of $IC_{50}$ was recorded in the PEGylated formulation. The statistical evaluation using two-way ANOVA with Dunnett's multiple comparisons showed that the PDT effect produced by different light fluences differed significantly ($p < 0.0001$) to the unirradiated samples (dark control).

In order to evaluate the photodynamic effect produced by mTHPC after activation at a different wavelength, all the formulations were irradiated with a series of light fluences at a wavelength of $\lambda = 457$ nm. Similar to previous studies [37], free mTHPC (dissolved in DMSO) produced dark toxicity but none of the liposomal formulations affected the cell viability without application of the fluence [36]. When irradiated with a light dose of 1 $Jcm^{-2}$, only liposome comprising DPPC/DPPE-$mPEG_{5000}$ was able to reduce the cell viability to 52% compared to the photo-toxicity produced by free mTHPC. This could be attributed to the presence of smaller liposomes with some disk-like associates in the formulation. They can be quickly taken up by the cells and the photosensitizer can be released readily resulting in the immediate burst effect [32]. By further increasing the fluence level, the cell viability gradually decreased to 20% in all the formulations at a light dose of 10 $Jcm^{-2}$ (Fig. 3). It was evident from the cell viability data obtained from photodynamic therapy, that in order to produce a comparable photodestruction effect as produced by 1 $Jcm^{-2}$ (when irradiated at 652 nm), a ten-fold higher fluence (i.e. 10 $Jcm^{-2}$) was required (when irradiated at 457 nm). This could be credited to higher light absorption, increased penetration depth (i.e. 2–3 mm as compared to 0.3 mm in blue light) as well as the higher quantum yield of light at longer wavelength region (i.e. red) as described by Kiesslich et al [38].

### 3.5. Hemocompatibility

Hemocompatibility studies serve as a critical link between *in vitro* and *in vivo* studies because the data obtained from these studies can be used to tailor the dosage form for the *in vivo* experiments [39]. Hemolysis assay was used to investigate the extent of erythrocyte destruction induced by the liposomal formulations and was conducted by estimating the amount of hemoglobin released after erythrocyte damage. This hemoglobin is then converted to oxyhemoglobin in the presence of atmospheric oxygen. The oxyhemoglobin can be detected and measured spectrophotometrically. This assay can be used to determine the safe concentrations that can be administered intravenously [14]. In our study, the hemocompatibility was observed for the first time for mTHPC and its liposomal formulations and the results indicated that all the mTHPC loaded liposomal formulations exhibit very low hemolytic properties as compared to the free drug dissolved in 0.1% DMSO (Fig. 4A). The hemolysis potential expressed by all the formulation was below 10% while the free drug showed a relatively higher hemolytic effect (i.e. 25%). Activated partial thromboplastin time (aPTT) was performed to evaluate the effect of liposomal formulation on the coagulation time. The coagulation time of all the formulations was found to between 30 and 40 s which was well under the standard range. aPTT values above 50 s are clinically significant while the value above 70 s indicates the continuous bleeding and hemorrhage. The free drug exhibited a higher coagulation time of 47 s (Fig. 4B). These findings suggested that our mTHPC loaded liposomal formulations are suitable for i.v. injection with a low possibility to induce bleeding and as discussed in Section 3.4 non-toxic as well.

### 3.6. Cellular uptake studies

The cellular uptake and intracellular distribution of free and liposome-bound mTHPC were evaluated using CLSM (Fig. 5). Therefore, SK-OV-3 cells were incubated with the different liposomal formulations (5 μM) at 37 °C for 2 h. A considerable localization of mTHPC was observed in both dark and irradiated samples. The red fluorescence of mTHPC loaded liposomes could be readily detected as a diffuse signal throughout the cytoplasm with particularly intense localization in the perinuclear region. The fluorescence distribution of the intracellular mTHPC did not show any significant difference between the liposomal formulations and free mTHPC (dissolved in 0.1% DMSO). The cells were counterstained with Sytox green™ (50 nM) and were observed as a

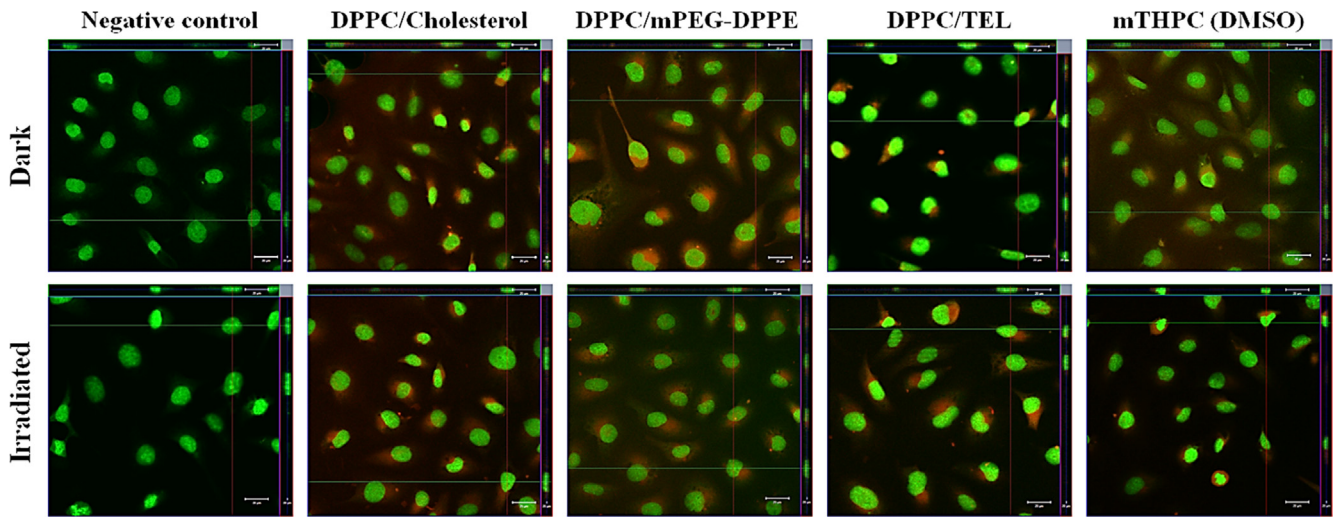


**Fig. 5.** CLSM micrographs of SK-OV-3 cells incubated with 5 μM mTHPC loaded liposomes and free mTHPC (dissolved in 0.1% DMSO) for 2 h at 37 °C. The cells were subsequently irradiated at 652 nm with a radiation fluence of 0.05 $Jcm^{-2}$. The untreated cells were taken as negative control (NC). The nucleus was counterstained using Sytox green™ (50 nM). The cellular uptake was observed using fluorescence detection filters for Sytox green™ (ex/em 504/523 nm) and mTHPC (ex/em. 420/652 nm). The scale bar represents 20 μm scale. (For interpretation of the references to colour in this figure legend, the reader is referred to the web version of this article.)

green fluorescent signal in the nuclear region. The co-localization of red and green fluorescence in the merge channel showed no sign of mTHPC localization in the nucleus. From the CLSM micrographs, it was observed that PEG-PE based liposome showed a comparable intracellular localization as that of free mTHPC which can be attributed to higher uptake of the combination of disk-like associates as mentioned in Section 3.3 and liposomes present in PEG-PE based formulation. On the basis of these observations, it was inferred that intracellular activation of mTHPC leads to the destruction of subcellular organelles resulting in cell death. Confocal microscopy also proved that a comparable fluorescence was emitted from the individual cells, which indicated the uniform uptake of mTHPC by the cells. This examination could be an important prerequisite for an effective PDT in tumor tissue, focusing on the complete destruction of cancer cells.

### 3.7. Determination of cellular reactive oxygen species (cROS)

In order to quantify the cROS generation and oxidative stress during the photodynamic treatment of the SK-OV-3 cells, the ROS assay was performed. It is based on cellular esterase-mediated hydrolysis of acetate group and intracellular oxidation of non-fluorescent $H_2$DCFDA (2‘,7‘-dichlorodihydrofluorescein) into green fluorescent DCF (2′,7′-Dichlorfluorescein). The data obtained from the photodynamic mediated production of ROS is shown in Fig. 6. In our experiments, the irradiated liposomal formulations produced increased levels of intracellular ROS as compared to non-irradiated ones (dark). The highest amount of ROS was produced by PEGylated liposomes owing to the presence of mixed structures as discussed in 3.3 in the formulation resulting in the higher uptake of the PEG-PE based structures [32]. Because of their smaller size, they exhibit a spontaneous penetration into the interstitium of tumor vasculature due to enhanced permeability and retention effect. Diffusion and accumulation parameters of the drug carriers in tumors have been shown to be highly dependent on their cut off size. According to Blanco et al. [40] the higher uptake of these mixed structures, in turn, deliver increased quantities of the drug to the tumor resulting in higher cytotoxicity. It indicates the liposomes containing DPPE-$mPEG_{5000}$ caused the highest damage to the cell as compared to other liposomal formulations. Nevertheless, in both experiments, cells were irradiated at the same energy level with different wavelengths, but the amount of ROS produced was higher when irradiated with the red light. These results were also in line with the results obtained from the cell viability assay. It can be suggested that the production of ROS is very crucial for an effective photodynamic treatment of cancer cells (see Fig. 7).

### 3.8. Vascular targeted PDT for photo-destruction of CAM microvasculature

The chorioallantoic membrane as a cost effective and less sentient *in vivo* model was used to evaluate the efficacy of the delivery system. The CAM is a highly vascularized tissue of the avian embryo containing both mature vessels as well as the capillaries. The vessel diameters in the CAM ranges from 20 to 120 μm which is comparable to the typical diameters of neovasculature in tumors. The CAM serves as a specialized respiratory tissue that allows for nutrient, ion and gaseous exchange between the embryo and the atmosphere surrounding the egg. This model offers several advantages for the evaluation of DDS incorporating PS. The CAM is easily accessible and easy to handle for administration and irradiation of PS without initiating an immune reaction from the developing embryo [41]. Because of the transparency of its superficial layers, PDT-induced vascular damage can be monitored in real-time as in individual blood vessels (usually within 3 h). The use of *in vivo* CAM model also helps reduce the use of animal models for the formulation testing. This model has also been approved by FDA as a pre-clinical protype for the biomaterial evaluations. The vascular targeted photodestruction of CAM is an important connection towards the targeting of tumor microvasculature thereby destroying the tumor tissue. To determine the extent of damage to the vasculature, PDT to the CAM was performed. In our experiments, it was observed that injection of the empty liposomes or normal saline only, did not produce any changes to the vasculature. Also, the additional application of the light dose to the CAM without prior treatment with liposomal formulations did not affect the integrity and profusion of the vasculature. To distinguish the changes in blood flow within CAM, 100 μl of mTHPC loaded liposomes (diluted in PBS) were injected intravenously followed by irradiation of the injection site. It was observed that the time past injection, the drug-light interval (DLI), plays a vital role in the photo-destruction of CAM vessels. Short DLI (e.g. 15 or 30 min) did not produce any effect and CAM vasculature remained somewhat intact. But when the irradiation was performed 1 h post liposomes injection, a delayed local destruction of CAM vasculature was observed within the irradiated area. Typical micrographs of CAM at different time periods after I.V injection based on mTHPC encapsulated liposomes are demonstrated in Fig. 8.

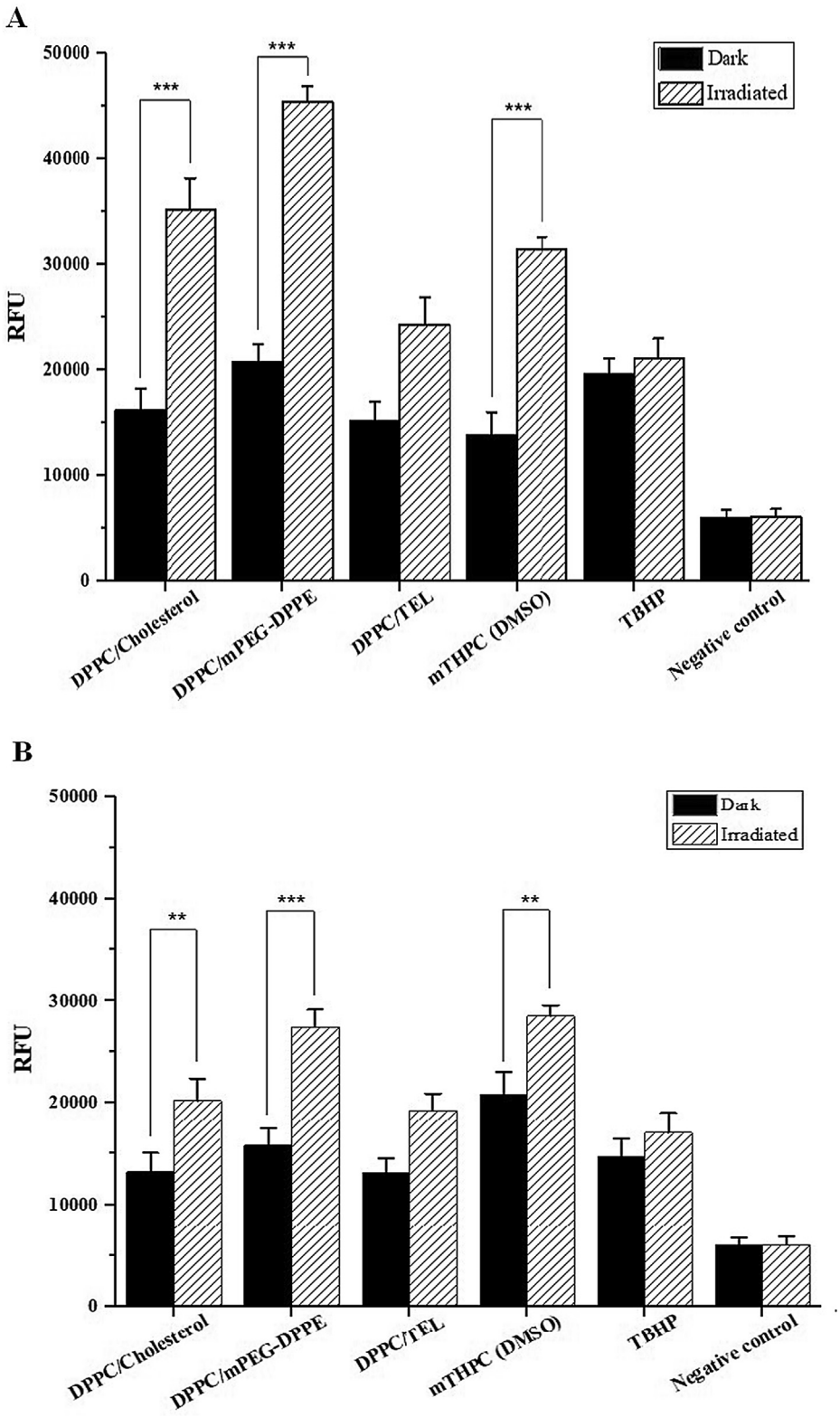


**Fig. 6.** Production of reactive oxygen species after dark (black bars) and photodynamic treatment (light grey bars) of SK-OV-3 cells with mTHPC loaded liposomes. Following 2 h incubation SK-OV-3 cells were irradiated at a light dose of 1 $Jcm^{-2}$ (A) $\lambda = 652$ nm and (B) $\lambda = 457$ nm. TBHP (50 μM) was used as a positive control. All the measurements were performed in triplicate and values were expressed as mean ± SD (n = 3).

Nevertheless, all the formulations showed mild closure of smaller capillaries that onset at $t_{post}$ = 10 min (data not shown), the larger vessels still remain unscathed and intermittent blood flow was observed. The effect was more pronounced in liposome comprising of DPPC/DPPE-$mPEG_{5000}$. However, at $t_{post}$ = 60 min, a complete occlusion of large vessels with the characteristic decline in blood flow was visible. These findings were in line with the previous observations regarding *in-ovo* PDT [11]. Ultimately at 24 h after treatment ($t_{post}$ = 24 h), a complete destruction of CAM vasculature at the irradiated area was evident. Scar formation due to the effective closure of all the blood vessels was

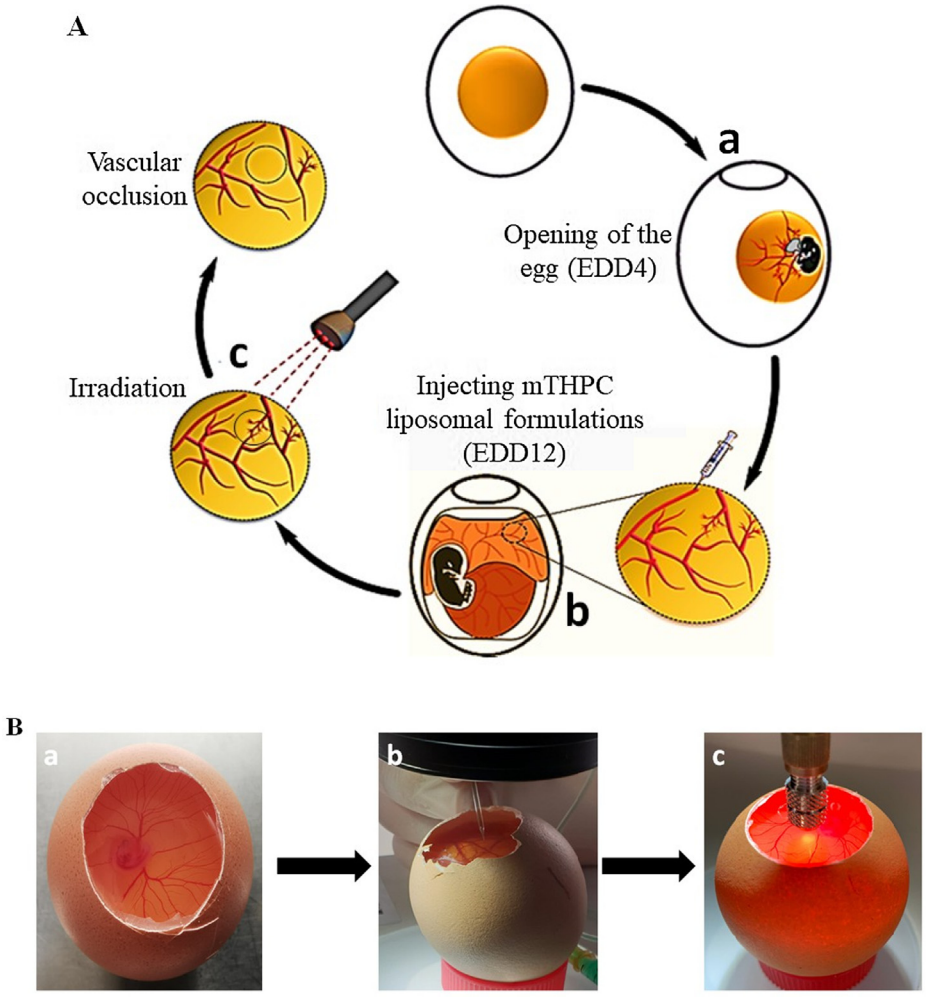


**Fig. 7.** (A) Schematic illustration and (B) An experimental illustration of vascular occlusion to the CAM; (a) The opened egg (EDD4) (b) Injecting mTHPC liposomal formulations to the CAM vessels (EDD12) (c) Irradiation of the CAM vasculature after incubations for 1 h.

observed in the CAM after 24 h while the embryo still survived (data not shown). There was a mild or no effect observed when free mTHPC (dissolved in PBS/DMSO) was injected. This could be attributed to the dimerization of drug molecules that resulted in the reduction of its efficacy.

### 3.9. Serum protein interaction with liposomes

In order to determine the effect of serum on the structural integrity of liposomal formulations, stability studies were conducted. Liposomal stability can be the measured with the extent to which entrapped agents are retained by the liposomes. It depends not only on the physical characteristics of the encapsulated agent and the carrier system but also on the biological environment with which these liposomes come in contact. The absorption of serum proteins on the liposomal carriers was estimated by measuring the change in liposome size. The data obtained by the stability studies of mTHPC loaded formulations in PBS (pH 7.4) is shown in Table 3 and for FCS (60%) in Table 4 respectively. It was observed the incubation of liposomal formulations with 60% of serum for 24 h resulted in an increased PDI and consequently reduced homogeneity of all the liposomal formulations. The changes in PDI were independent of the liposomal size [42]. The highest change of PDI was observed in TEL containing liposomes. Zeta potential of the liposomes decreased when incubated with serum as compared to the zeta potential when incubated in PBS (pH 7.4). This is attributed to the fact that the charged particles adsorb more proteins on their surface than the neutral ones that result in the reduction of the zeta potential [43]. The hydrodynamic diameter of liposomes was also reduced after 24 h incubation in serum. This effect was more pronounced in non-PEGylated liposomes as compared to PEGylated-liposomes. This is due to the fact that the serum interacts with liposomes caused by the adsorption of the proteins on the liposome surface forming a “protein corona”. The serum proteins are impermeable to the liposomal membrane and due to osmotic pressure, the escape of water from the liposomal core resulting in the shrinkage of the liposome size [42,43]. A relatively less effect was noticed in liposomes containing PEG in small molar fractions. This effect can be attributed to the fact that liposomes with PEG chains not only hinders the interaction with serum proteins due to repulsive forces resulting in less dense protein corona but also suppress the recognition by opsonins due to high flexibility and hydrophilicity of the PEG chains in the serum [44].

### 3.10. Single cell gel electrophoresis

The photodynamic treatment of cells can cause a genotoxicity effect. Therefore, the comet assay, a cytogenic technique used mainly in the field of toxicological studies, was recently established in the assessment of this type of toxicity. The alkaline version of the comet assay is a simple and rapid *in vitro* screening method for analyzing and measuring the DNA single-strand breaks (SSB) or alkali labile sites [45]. The principle of the comet assay is based on the fact that DNA strands which occur as a negatively charged supercoiled structure in the nucleus can

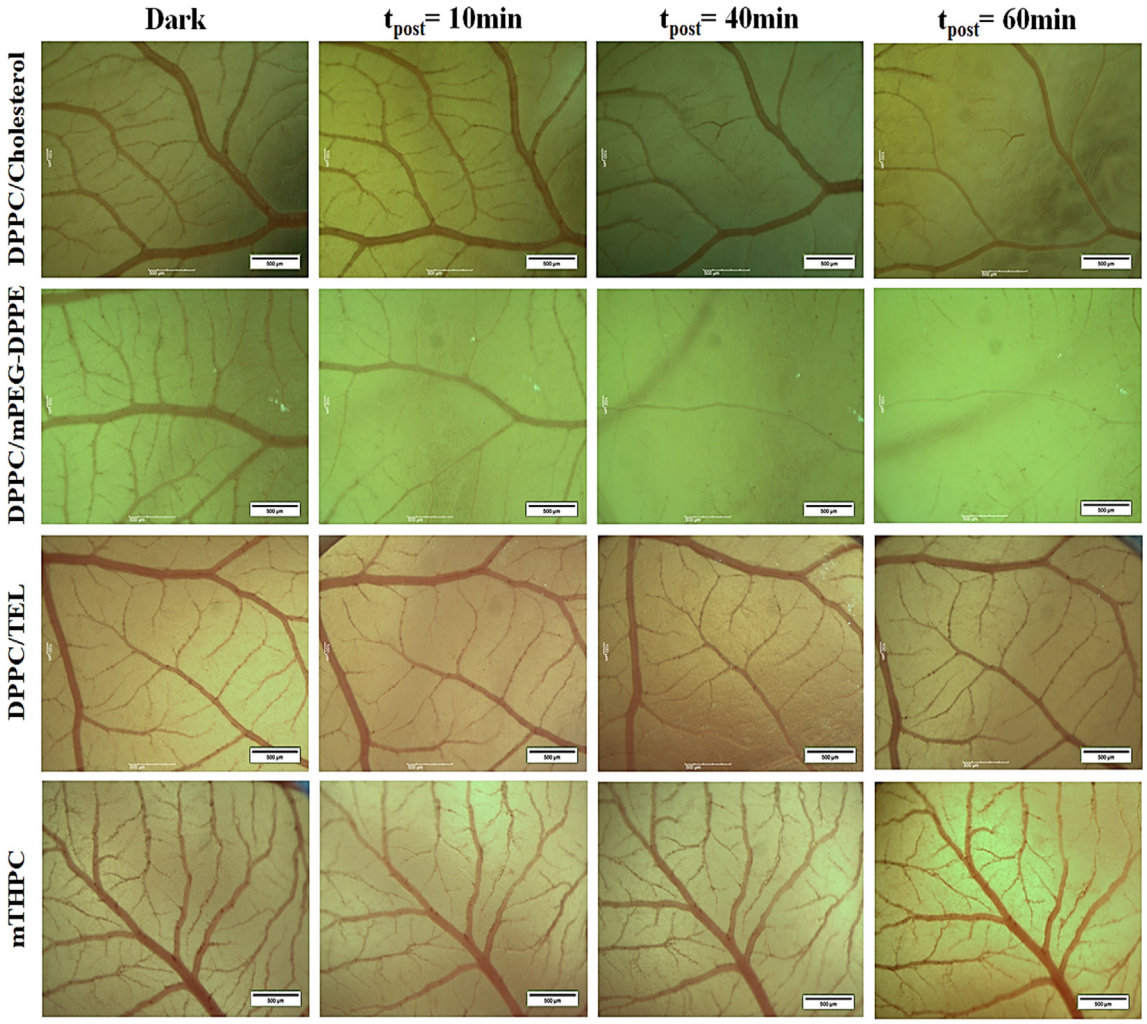


**Fig. 8.** Typical stereomicrographs of CAM representing PDT mediated occlusion of CAM vasculature. Images were acquired before (dark), immediately after irradiation ($t_{post}$ = 0 min) and at $t_{post}$ 10, 40- and 60-min post I.V injection of mTHPC loaded liposomes (0.5 mg mTHPC/10 mg of lipids). Irradiation was performed at a light dose of 4.8 $Jcm^{-2}$ using a red laser diode (652 nm, 40 mW) with Weber needle. The scale bar represents the 500 μm scale. (For interpretation of the references to colour in this figure legend, the reader is referred to the web version of this article.)

**Table 3**
Stability studies of mTHPC encapsulated liposomes (0.5 mg mTHPC/10 mg total lipid) after incubation with PBS (pH 7.4; without $Ca^{2+}/Mg^{2+}$) for 24 h. Hydrodynamic diameter is expressed as particles size distribution by intensity (n = 3).

| Liposomal Formulation (mol %) | Time (h) | Diameter (nm) ± SD | PDI ± SD | Surface Charge (mV) ± SD |
|---|---|---|---|---|
| DPPC/Chol.-mTHPC (90:10) | 0 | 126.7 ± 5.4 | 0.15 ± 0.04 | −5.4 ± 0.8 |
| | 1 | 123.9 ± 4.0 | 0.15 ± 0.03 | −2.8 ± 0.6 |
| | 4 | 131.9 ± 11.6 | 0.17 ± 0.06 | −3.4 ± 1.1 |
| | 24 | 135.4 ± 11.7 | 0.20 ± 0.06 | −5.9 ± 3.3 |
| DPPC/$mPEG_{5000}$-DPPE-mTHPC (95:5) | 0 | 139.7 ± 7.5 | 0.18 ± 0.06 | −5.6 ± 1.4 |
| | 1 | 122.4 ± 12.5 | 0.20 ± 0.07 | −2.6 ± 1.0 |
| | 4 | 150.0 ± 12.9 | 0.24 ± 0.01 | −5.5 ± 4.3 |
| | 24 | 146.7 ± 20.9 | 0.23 ± 0.01 | −4.0 ± 1.4 |
| DPPC/TEL-mTHPC (90:10) | 0 | 97.6 ± 3.2 | 0.27 ± 0.01 | −5.9 ± 0.9 |
| | 1 | 95.9 ± 1.6 | 0.25 ± 0.01 | −7.4 ± 0.7 |
| | 4 | 103.5 ± 1.4 | 0.28 ± 0.01 | −7.7 ± 0.7 |
| | 24 | 110.5 ± 2.4 | 0.43 ± 0.01 | −9.9 ± 0.2 |

be fragmented due to the exposure to the toxins or drug treatments. These DNA SSBs are drawn towards anode under the influence of the electric field and appear as the olive tail. The measure of this tail moment is identified as the index of DNA damage. Due to the fact that photosensitizers upon administration may also accumulate into the normal tissue and may cause complications under low light dose or normal light (i.e. room or sunlight) [46]. Form Fig. 9, it can be observed that no direct DNA strand breakage was caused by photodynamic treatment of mTHPC encapsulated liposomes as observed from the olive tail moment data. From the data, it was inferred that irradiation of the SK-OV-3 cells after treatment with a low drug or light dose (0.05 $Jcm^{-2}$) did not cause any significant DNA damage and there was no apparent increase in the olive tail. Also, it was observed that there was no DNA damage in the absence of light (data not shown). From the above-mentioned results, it can be assumed that mTHPC can be used clinically with no or minimum incidence of genetic toxicity [27].

### 3.11. Cellular uptake pathway analysis

To study the internalization mechanism of mTHPC loaded liposomes in the SK-OV-3 cells, the inhibitors of the cellular uptake pathways were used. Two major pathways utilized for the internalization of the nanocarriers includes the clathrin-dependent endocytosis and caveolin dependent pathway. Clathrin dependent endocytosis is selectively obstructed by Chlorpromazine which acts by inhibiting the formation of clathrin-coated vesicles that are formed by the clathrin-coated pits leading to the formation of endosomes that ultimately fuse with

**Table 4**
Stability studies of mTHPC encapsulated liposomes (0.5 mg mTHPC/10 mg total lipid) after incubation with FCS for 24 h. Hydrodynamic diameter is manifested as a function of serum absorption on the liposomal surface and expressed as particle size distribution by intensity (n = 3).

| Liposomal Formulation (mol %) | Time (h) | Diameter (nm) ± SD | PDI ± SD | Surface Charge (mV) ± SD |
|---|---|---|---|---|
| DPPC/Chol.-mTHPC (90:10) | 0 | 126.7 ± 5.4 | 0.15 ± 0.04 | −5.4 ± 0.8 |
| | 1 | 108.3 ± 1.7 | 0.18 ± 0.01 | −8.8 ± 0.8 |
| | 4 | 116.9 ± 4.5 | 0.20 ± 0.03 | −8.5 ± 1.2 |
| | 24 | 112.7 ± 6.5 | 0.20 ± 0.03 | −9.5 ± 0.7 |
| DPPC/$mPEG_{5000}$-DPPE-mTHPC (95:5) | 0 | 139.7 ± 7.5 | 0.18 ± 0.06 | −9.6 ± 1.4 |
| | 1 | 103.2 ± 2.1 | 0.27 ± 0.01 | −5.2 ± 0.5 |
| | 4 | 113.5 ± 8.5 | 0.26 ± 0.03 | −5.0 ± 0.8 |
| | 24 | 129.7 ± 2.4 | 0.32 ± 0.03 | −11.7 ± 0.9 |
| DPPC/TEL-mTHPC (90:10) | 0 | 107.5 ± 1.1 | 0.25 ± 0.02 | −9.9 ± 0.5 |
| | 1 | 108.1 ± 1.7 | 0.39 ± 0.01 | −10.5 ± 0.6 |
| | 4 | 125.5 ± 3.8 | 0.36 ± 0.01 | −10.5 ± 0.6 |
| | 24 | 95.73 ± 2.5 | 0.40 ± 0.01 | −11.4 ± 0.4 |

lysosomes. Caveolin dependent mechanism is inhibited by Filipin-III. It is a macrolide antibiotic that acts by interfering with cholesterol mediated endocytic functions thereby inhibiting the lipid raft or caveolae endocytosis [47]. Fig. 10 demonstrates that the incubating the cells without any formulation (i.e. mTHPC loaded liposomes) and/or with inhibitors did not show any decrease in the cell viability. The cells incubated with mTHPC loaded liposomes without any inhibition showed a substantial reduction in the cell viability after irradiation. Furthermore, when the cells were preincubated with chlorpromazine, a considerable increase in the cell viability was observed due to the inhibition of liposome uptake. Additional incubation with Filipin-III showed relatively less inhibition of liposomal uptake. This inference leads to the presumption that liposomal uptake occurs mainly through clathrin-mediated endocytosis. None of the inhibitors was able to minimize the uptake of the free mTHPC (dissolved in DMSO). This result leads to the inference that the free drug is not internalized by any of the said mechanisms. Instead, it is taken up by the cells through the diffusion process. These findings are in agreement with the earlier studies elaborating that the lipid particles are mainly internalized via clathrin-dependent pathways and are highly dependent on cell type [48].

## 4. Conclusion

In order to reduce the aggregation effect and to improve the monomerization of mTHPC, novel liposomal drug carrier systems were developed. These nanocarriers not only enhance its distribution in the lipid bilayer resulting in the increased stability, but also improve its efficacy against the cancer cells. Effective drug loading was confirmed by encapsulation efficiency which was more than 75% in all the cases. These formulations did not cause any dark toxicity and prompted the dose-dependent destruction of cancer cells upon irradiation of PS inside the cells using a prototype LED device. The highest photodynamic effect was produced by the liposomes containing DPPE-$mPEG_{5000}$ as a small molar fraction. This observation leads to the conclusion that the presence of small liposomes along with mixed micelles in the formulation can be more effective not only in the treatment of cancer but also

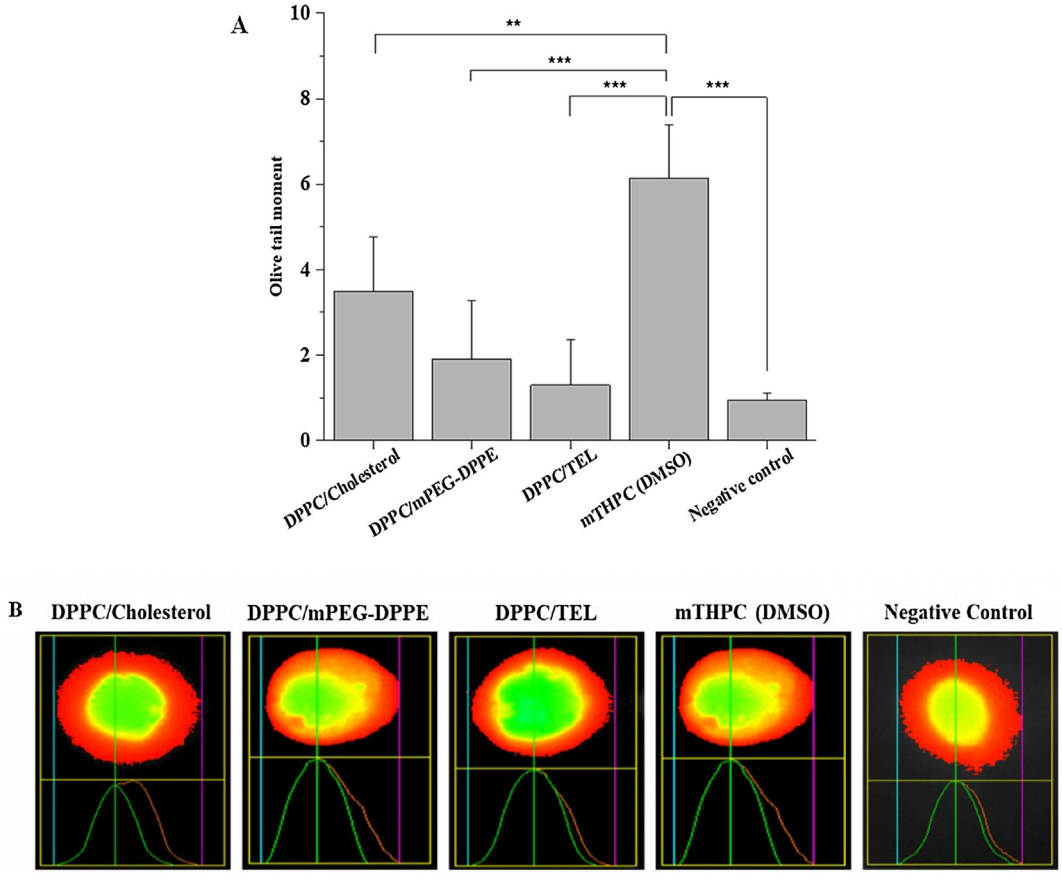


**Fig. 9.** (A) Distribution of comet tail moment & (B) Fluorescence micrographs of genotoxicity to SK-OV-3 cells obtained from alkaline Comet assay. The cells were incubated with mTHPC loaded liposomes for 2 h at an equitoxic dose to produce 80% cell viability to avoid false-positive response. Irradiation was performed at a light dose of 0.05 $Jcm^{-2}$. Each value is represented as the mean ± SD for three independent experiments. For the statistical analysis, the comparison was done against the dark treatment. P values ($p < 0.05$) were considered significant and denoted as '****' ($p < 0.0001$) and '**' ($p < 0.01$).

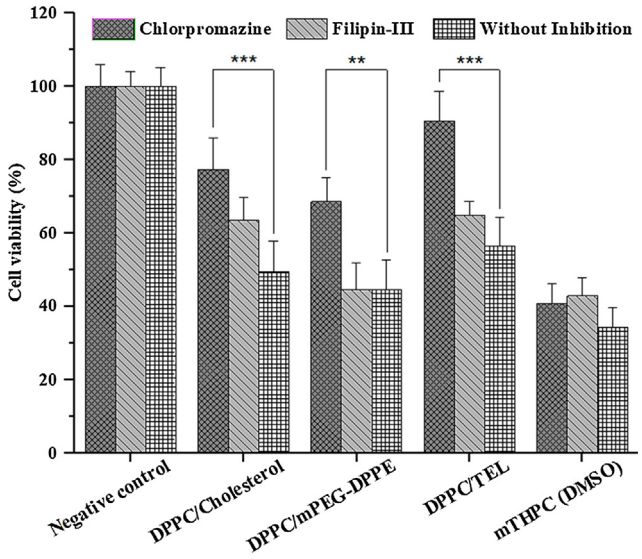


**Fig. 10.** The cell viability of the SK-OV-3 cells after incubation with mTHPC loaded liposomes (1.5 μM) and free mTHPC (dissolved in DMSO). The endocytic pathways were inhibited by pre-incubation with Chlorpromazine (30 μM) and Filipin-III (15 μM) for 1 h. The unirradiated cells were considered as blank control. The values are represented as the mean ± SD for three independent experiments.

provides the stealth effect against opsonization. A reasonable molar fraction of TELs in the liposomes stabilized the liposomal membrane. This effect can be exploited to control the release of drug from the liposome for longer durations. Intracellular delivery of the PS was confirmed by confocal microscopy, which revealed the effective localization of mTHPC into the cytoplasm. This also suggested that mTHPC produced its effect by the production of ROS, which caused the disruption of intracellular organelle structures. When PS activation with different wavelengths was compared, it was observed that activation with red light ($\lambda = 652$ nm) produced a pronounced effect even at low light fluence as compared to the PS activation with blue light ($\lambda = 457$ nm). *In-vivo* chick CAM demonstrated successful local vascular occlusion at the irradiated area with no effect on developing embryo. This approach can serve as an effective strategy to target the tumor vasculature in the *in vivo* tumor model. The comet assay showed no incidence of genotoxicity. Serum and plasma stability studies illustrated the complete biocompatibility of liposomal formulations. Therefore, on the basis of these results, it can be inferred that our nanoformulations are the promising candidates in-terms of safety and efficacy in the treatment of cancer disorders.

## Acknowledgment:

We would like to thank Mrs. Eva Mohr, Department of Pharmaceutics and Biopharmaceutics, Philipps University Marburg, for technical work and kind support throughout the research period. The authors would also like to express their gratitude to the German academic exchange service and Higher education commission of Pakistan (DAAD/HEC) for providing the scholarship.

## References

[1] N.R. Jabir, S. Tabrez, G.M. Ashraf, S. Shakil, G.A. Damanhouri, M.A. Kamal, Nanotechnology-based approaches in anticancer research, Int. J. Nanomed. 7 (2012) 4391–4408.
[2] C.M. Moore, D. Pendse, M. Emberton, Photodynamic therapy for prostate cancer—a review of current status and future promise, Nat. Rev. Urol. 6 (2009) 18–30.
[3] W. Peng, D.F. Samplonius, S. de Visscher, J.L. Roodenburg, W. Helfrich, M.J. Witjes, Photochemical internalization (PCI)-mediated enhancement of bleomycin cytotoxicity by liposomal mTHPC formulations in human head and neck cancer cells, Lasers Surg. Med. 46 (2014) 650–658.
[4] A. Petri, D. Yova, E. Alexandratou, M. Kyriazi, M. Rallis, Comparative characterization of the cellular uptake and photodynamic efficiency of Foscan® and Fospeg in a human prostate cancer cell line, Photodiagn. Photodyn. Ther. 9 (2012) 344–354.
[5] M.O. Senge, mTHPC–A drug on its way from second to third generation photosensitizer? Photodiagn. Photodyn. Ther. 9 (2012) 170–179.
[6] M.J. Bovis, J.H. Woodhams, M. Loizidou, D. Scheglmann, S.G. Bown, A.J. MacRobert, Improved in vivo delivery of m-THPC via pegylated liposomes for use in photodynamic therapy, J. Control. Release 157 (2012) 196–205.
[7] A. Nagayasu, K. Uchiyama, H. Kiwada, The size of liposomes: a factor which affects their targeting efficiency to tumors and therapeutic activity of liposomal antitumor drugs, Adv. Drug Deliv. Rev. 40 (1999) 75–87.
[8] K.H. Engelhardt, S.R. Pinnapireddy, E. Baghdan, J. Jedelská, U. Bakowsky, Transfection studies with colloidal systems containing highly purified bipolar tetraether lipids from sulfolobus acidocaldarius, Archaea 2017 (2017) 8047149.
[9] G. Mahmoud, J. Jedelská, S.M. Omar, B. Strehlow, M. Schneider, U. Bakowsky, Stabilized tetraether lipids based particles guided porphyrins photodynamic therapy, Drug Delivery 25 (2018) 1526–1536.
[10] J. Schäfer, S. Höbel, U. Bakowsky, A. Aigner, Liposome–polyethylenimine complexes for enhanced DNA and siRNA delivery, Biomaterials 31 (2010) 6892–6900.
[11] G. Mahmoud, J. Jedelská, B. Strehlow, S. Omar, M. Schneider, U. Bakowsky, Photoresponsive tetraether lipids based vesicles for prophyrin mediated vascular targeting and direct phototherapy, Colloids Surf., B 159 (2017) 720–728.
[12] N. Plenagl, B.S. Seitz, S. Reddy Pinnapireddy, J. Jedelská, J. Brüßler, U. Bakowsky, Hypericin loaded liposomes for anti-microbial photodynamic therapy of gram-positive bacteria, Phys. Status Solidi (a) 215 (2018) 1700837.
[13] N. Plenagl, L. Duse, B.S. Seitz, N. Goergen, S.R. Pinnapireddy, J. Jedelska, J. Brüßler, U. Bakowsky, Photodynamic therapy–hypericin tetraether liposome conjugates and their antitumor and antiangiogenic activity, Drug Delivery 26 (2019) 23–33.
[14] L. Duse, S.R. Pinnapireddy, B. Strehlow, J. Jedelská, U. Bakowsky, Low level LED photodynamic therapy using curcumin loaded tetraether liposomes, Eur. J. Pharm. Biopharm. 126 (2018) 233–241.
[15] J. Sitterberg, A. Özcetin, C. Ehrhardt, U. Bakowsky, Utilising atomic force microscopy for the characterization of nanoscale drug delivery systems, Eur. J. Pharm. Biopharm. 74 (2010) 2–13.
[16] B.S. Seitz, N. Plenagl, M. Raschpichler, H. Vögeling, M. Wojcik, S.R. Pinnapireddy, J. Brüßler, U. Bakowsky, Nanoparticles and liposomes for the surface modification of implants: a comparative study of spraying and dipping techniques, Phys. Status Solidi (a) 215 (2018) 1700847.
[17] C. Janich, S. Taßler, A. Meister, G. Hause, J. Schäfer, U. Bakowsky, G. Brezesinski, C. Wölk, Structures of malonic acid diamide/phospholipid composites and their lipoplexes, Soft Matter 12 (2016) 5854–5866.
[18] C. Yow, J. Chen, N. Mak, N. Cheung, A. Leung, Cellular uptake, subcellular localization and photodamaging effect of temoporfin (mTHPC) in nasopharyngeal carcinoma cells: comparison with hematoporphyrin derivative, Cancer Lett. 157 (2000) 123–131.
[19] L. Duse, E. Baghdan, S.R. Pinnapireddy, K.H. Engelhardt, J. Jedelská, J. Schaefer, P. Quendt, U. Bakowsky, Preparation and characterization of curcumin loaded chitosan nanoparticles for photodynamic therapy, Phys. Status Solidi (a) 215 (2018) 1700709.
[20] M. Raschpichler, M.R. Agel, S.R. Pinnapireddy, L. Duse, E. Baghdan, J. Schäfer, U. Bakowsky, In situ intravenous photodynamic therapy for the systemic eradication of bloodstream infections, Photochem. Photobiol. Sci. 18 (2019) 304–308.
[21] S.R. Pinnapireddy, L. Duse, B. Strehlow, J. Schäfer, U. Bakowsky, Composite liposome-PEI/nucleic acid lipopolyplexes for safe and efficient gene delivery and gene knockdown, Colloids Surf., B 158 (2017) 93–101.
[22] I. Tariq, S.R. Pinnapireddy, L. Duse, M.Y. Ali, S. Ali, M.U. Amin, N. Goergen, J. Jedelská, J. Schäfer, U. Bakowsky, Lipodendriplexes: a promising nanocarrier for enhanced gene delivery with minimal cytotoxicity, Eur. J. Pharm. Biopharm. 135 (2019) 72–82.
[23] G. Mahmoud, J. Jedelská, B. Strehlow, U. Bakowsky, Bipolar tetraether lipids derived from thermoacidophilic archaeon Sulfolobus acidocaldarius for membrane stabilization of chlorin e6 based liposomes for photodynamic therapy, Eur. J. Pharm. Biopharm. 95 (2015) 88–98.
[24] A. Özcetin, A. Aigner, U. Bakowsky, A chorioallantoic membrane model for the determination of anti-angiogenic effects of imatinib, Eur. J. Pharm. Biopharm. 85 (2013) 711–715.
[25] F. Bonté, R. Juliano, Interactions of liposomes with serum proteins, Chem. Phys. Lipids 40 (1986) 359–372.
[26] F.I. McNair, B. Marples, C.M. West, J.V. Moore, A comet assay of DNA damage and repair in K562 cells after photodynamic therapy using haematoporphyrin derivative, methylene blue and meso-tetrahydroxyphenylchlorin, Br. J. Cancer 75 (1997) 1721–1729.
[27] C. Yow, N. Mak, S. Szeto, J. Chen, Y. Lee, N. Cheung, D. Huang, A. Leung, Photocytotoxic and DNA damaging effect of temoporfin (mTHPC) and merocyanine 540 (MC540) on nasopharyngeal carcinoma cell, Toxicol. Lett. 115 (2000) 53–61.
[28] M. Hoebeke, X. Damoiseau, H.J. Schuitmaker, A. Van de Vorst, Fluorescence, absorption and electron spin resonance study of bacteriochlorin incorporation into membrane models, Biochim. Biophys. Acta (BBA)-Biomembr. 1420 (1999) 73–85.
[29] M. De Vetta, L. González, J.J. Nogueira, Hydrogen bonding regulates the rigidity of liposome-encapsulated chlorin photosensitizers, ChemistryOpen 7 (2018) 475–483.
[30] N. Dragicevic-Curic, M. Friedrich, S. Petersen, D. Scheglmann, D. Douroumis, W. Plass, A. Fahr, Assessment of fluidity of different invasomes by electron spin resonance and differential scanning calorimetry, Int. J. Pharm. 412 (2011) 85–94.
[31] Y. Li, L. Yang, Driving forces for drug loading in drug carriers, J. Microencapsul. 32

(2015) 255–272.
[32] M.C. Sandström, E. Johansson, K. Edwards, Structure of mixed micelles formed in PEG-lipid/lipid dispersions, Langmuir 23 (2007) 4192–4198.
[33] B. Ruozi, D. Belletti, A. Tombesi, G. Tosi, L. Bondioli, F. Forni, M.A. Vandelli, AFM, ESEM, TEM, and CLSM in liposomal characterization: a comparative study, Int. J. Nanomed. 6 (2011) 557–563.
[34] M. Almgren, K. Edwards, G. Karlsson, Cryo transmission electron microscopy of liposomes and related structures, Colloids Surf., A 174 (2000) 3–21.
[35] J. Kuntsche, J.C. Horst, H. Bunjes, Cryogenic transmission electron microscopy (cryo-TEM) for studying the morphology of colloidal drug delivery systems, Int. J. Pharm. 417 (2011) 120–137.
[36] K. Reidy, C. Campanile, R. Muff, W. Born, B. Fuchs, mTHPC-mediated photodynamic therapy is effective in the metastatic human 143B osteosarcoma cells, Photochem. Photobiol. 88 (2012) 721–727.
[37] E.V. Maytin, U. Kaw, M. Ilyas, J.A. Mack, B. Hu, Blue light versus red light for photodynamic therapy of basal cell carcinoma in patients with Gorlin syndrome: a bilaterally controlled comparison study, Photodiagn. Photodyn. Ther. 22 (2018) 7–13.
[38] T. Kiesslich, J. Berlanda, K. Plaetzer, B. Krammer, F. Berr, Comparative characterization of the efficiency and cellular pharmacokinetics of Foscan®-and Foslip®-based photodynamic treatment in human biliary tract cancer cell lines, Photochem. Photobiol. Sci. 6 (2007) 619–627.
[39] S. Pinnapireddy, L. Duse, D. Akbari, U. Bakowsky, Photo-enhanced delivery of genetic material using curcumin loaded composite nanocarriers, Clin. Oncol 2 (2017) 1323.
[40] E. Blanco, H. Shen, M. Ferrari, Principles of nanoparticle design for overcoming biological barriers to drug delivery, Nat. Biotechnol. 33 (2015) 941–951.
[41] D.O. DeFouw, V.J. Rizzo, R. Steinfeld, R.N. Freinberg, Mapping of the microcirculation in the chick chorioallantoic membrane during normal angiogenesis, Microvasc. Res. 38 (1989) 136–147.
[42] J. Wolfram, K. Suri, Y. Yang, J. Shen, C. Celia, M. Fresta, Y. Zhao, H. Shen, M. Ferrari, Shrinkage of pegylated and non-pegylated liposomes in serum, Colloids Surf., B 114 (2014) 294–300.
[43] J. Pencer, G.F. White, F.R. Hallett, Osmotically induced shape changes of large unilamellar vesicles measured by dynamic light scattering, Biophys. J. 81 (2001) 2716–2728.
[44] H.D. Han, B.C. Shin, H.S. Choi, Doxorubicin-encapsulated thermosensitive liposomes modified with poly (N-isopropylacrylamide-co-acrylamide): drug release behavior and stability in the presence of serum, Eur. J. Pharm. Biopharm. 62 (2006) 110–116.
[45] D.W. Fairbairn, P.L. Olive, K.L. O'Neill, The comet assay: a comprehensive review, Mutat. Res./Rev. Genetic Toxicol. 339 (1995) 37–59.
[46] L.C. Penning, K. Tijssen, J.P.J. Boegheim, J. van Steveninck, T.M. Dubbelman, Relationship between photodynamically induced damage to various cellular parameters and loss of clonogenicity in different cell types with hematoporphyrin derivative as a sensitizer, Biochim. Biophys. Acta (BBA)-Mol. Cell Res. 1221 (1994) 250–258.
[47] L. Duse, M.R. Agel, S.R. Pinnapireddy, J. Schäfer, M.A. Selo, C. Ehrhardt, U. Bakowsky, Photodynamic therapy of ovarian carcinoma cells with curcumin-loaded biodegradable polymeric nanoparticles, Pharmaceutics 11 (2019) 282–299.
[48] J. Rejman, A. Bragonzi, M. Conese, Role of clathrin-and caveolae-mediated endocytosis in gene transfer mediated by lipo-and polyplexes, Mol. Ther. 12 (2005) 468–474.